Thermal and Alignment Analysis of the Instrument-Level ATLAS Thermal Vacuum Test

Heather Bradshaw, NASA GSFC

Presented By

Heather Bradshaw

Thermal & Fluids Analysis Workshop
TFAWS 2012
August 13-17, 2012
Jet Propulsion Laboratory
Pasadena, CA

Outline

***Objective*: To design the thermal vacuum setup for the ATLAS test to adequately simulate flight-like conditions.**

- Mission Overview
  - ICESat-2 Spacecraft
  - ATLAS Instrument
- Design of TVac Test Setup
  - Location/Setpoints of Cryo Panels and Heater Panels
- STOP Analysis
  - Mapping Verification
  - Line of Sight (LOS) Results
- Conclusions

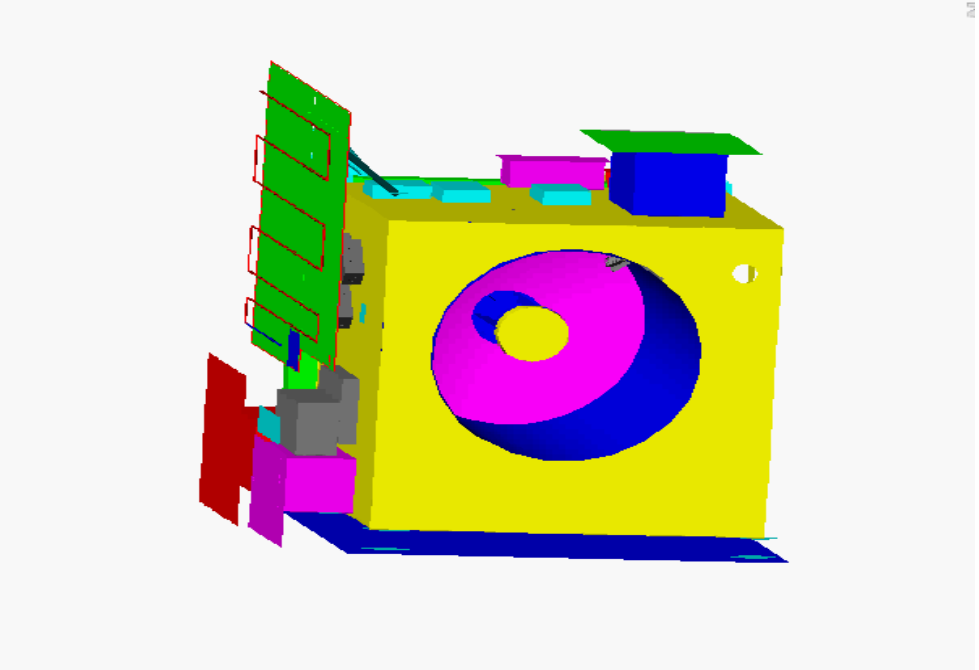

ATLAS Instrument

Note: STOP Analysis stands for Structural, Thermal, Optical Performance Analysis

Mission Overview

- **ICESat-2 Science Objectives**
  - Land Ice, Sea Ice, Vegetation
    - Quantify polar ice-sheet contributions to sea-level change
    - Estimate sea ice thickness
    - Measure vegetation canopy height, estimate biomass change
- **Mission Details**
    - Orbit: 496km, near-circular, near-polar
    - Mission Duration: 3 years (with propellant for 7 years)
    - Launch date: 2016
    - Single-instrument spacecraft
- **Acronyms**
  - ICESat-2
    - Ice, Cloud, and land Elevation Satellite-2 (ICESat-2)
  - ATLAS
    - Advanced Topographic Laser Altimeter System (ATLAS)

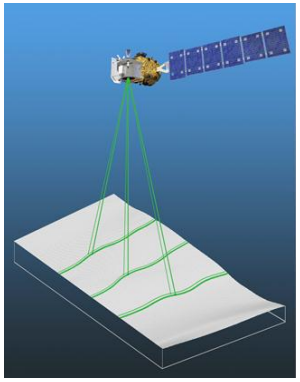

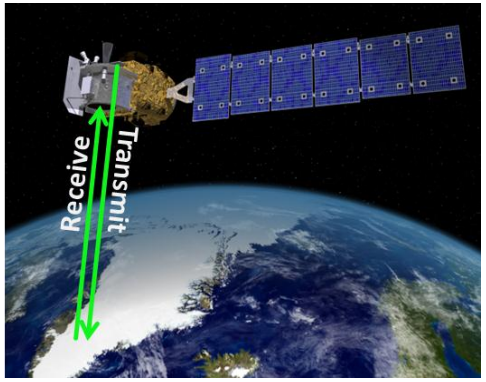

ICESat-2 Visualizations

- **ATLAS Instrument**
  - Laser
    - Wavelength: 532 nm (green light)
    - Single pulse, splits into 6 beams that form 3 strong/weak pairs
  - Operation
    - Transmit beams down to earth
    - Beams reflect and are received by telescope
    - Measure time of flight of each laser pulse

ATLAS Alignment Sensitivity

- Compared to other laser altimeters GSFC has built, the ATLAS beam has:
  - Smallest transmitted beam
  - Smallest receiver Field of View (FOV)
  - Smallest alignment margin
- Alignment Monitoring Control System (AMCS)
  - ATLAS has an active alignment system, which must be tested during thermal vacuum (TVac) environmental testing
- Why do STOP analysis for a thermal vacuum test?
  - STOP analysis usually reserved for flight predictions
  - ATLAS has unusually tight pointing requirements, and it is critical to simulate this flight-like pointing in test
- Novel aspects of ATLAS TVac test
  - Performing STOP analysis for TVac setup
  - Unique opportunity to verify STOP analysis results

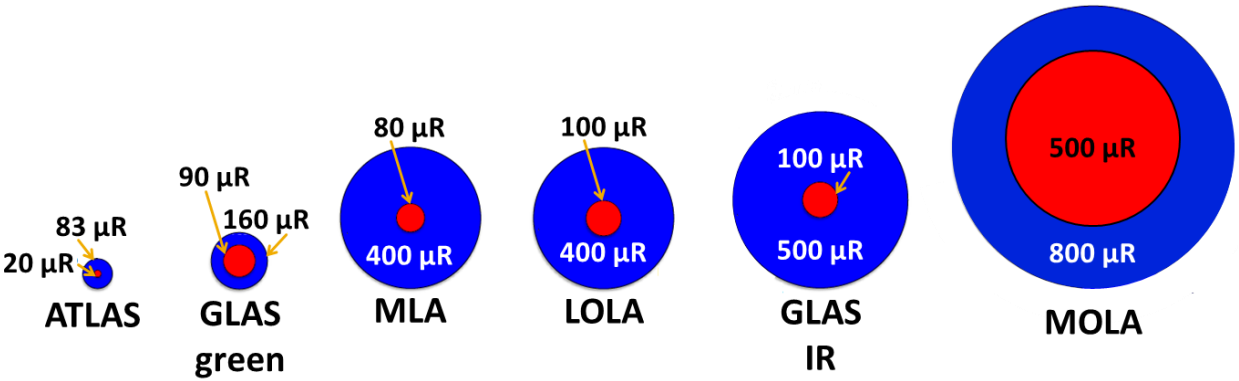

Comparison Between Laser Beam (red) and Receiver Field of View (blue) of Previous Laser Altimeters

DEMONSTRATION

Analysis Cases

- Four bounding cases selected for thermal balance test points:
  - Hot Cases
    - Hot Beta 0°
    - Hot Beta 70°
  - Cold Cases
    - Cold Beta 90° (nadir-pointing)
    - Cold Beta 90° Survival (solar-inertial)

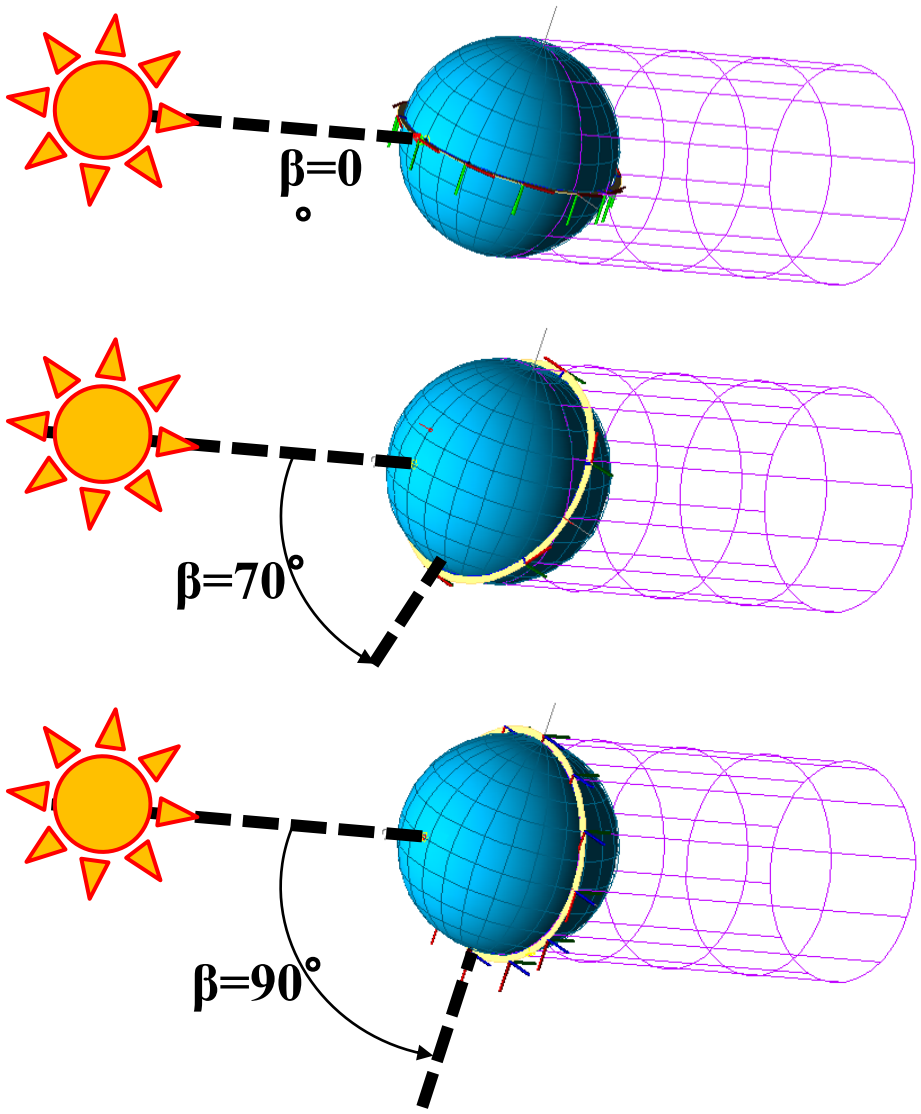

Note: Beta angle (β) is the angle between solar vector and orbit plane

Isometric View of Test Setup

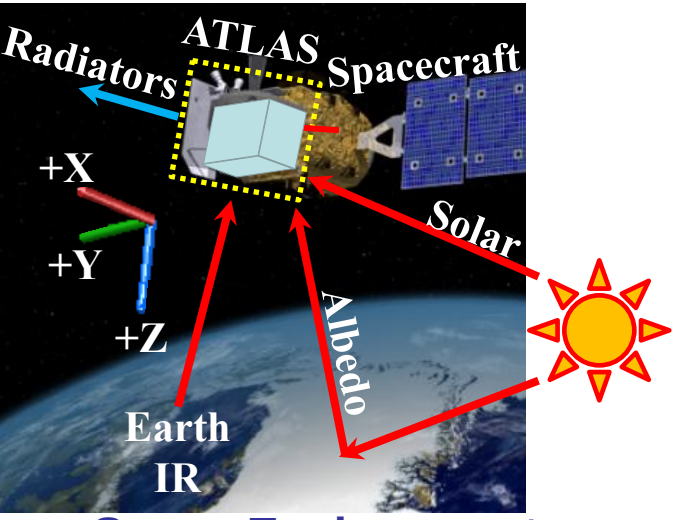

Space Environment to Simulate

Facility: Chamber 238

Test Date: 2015

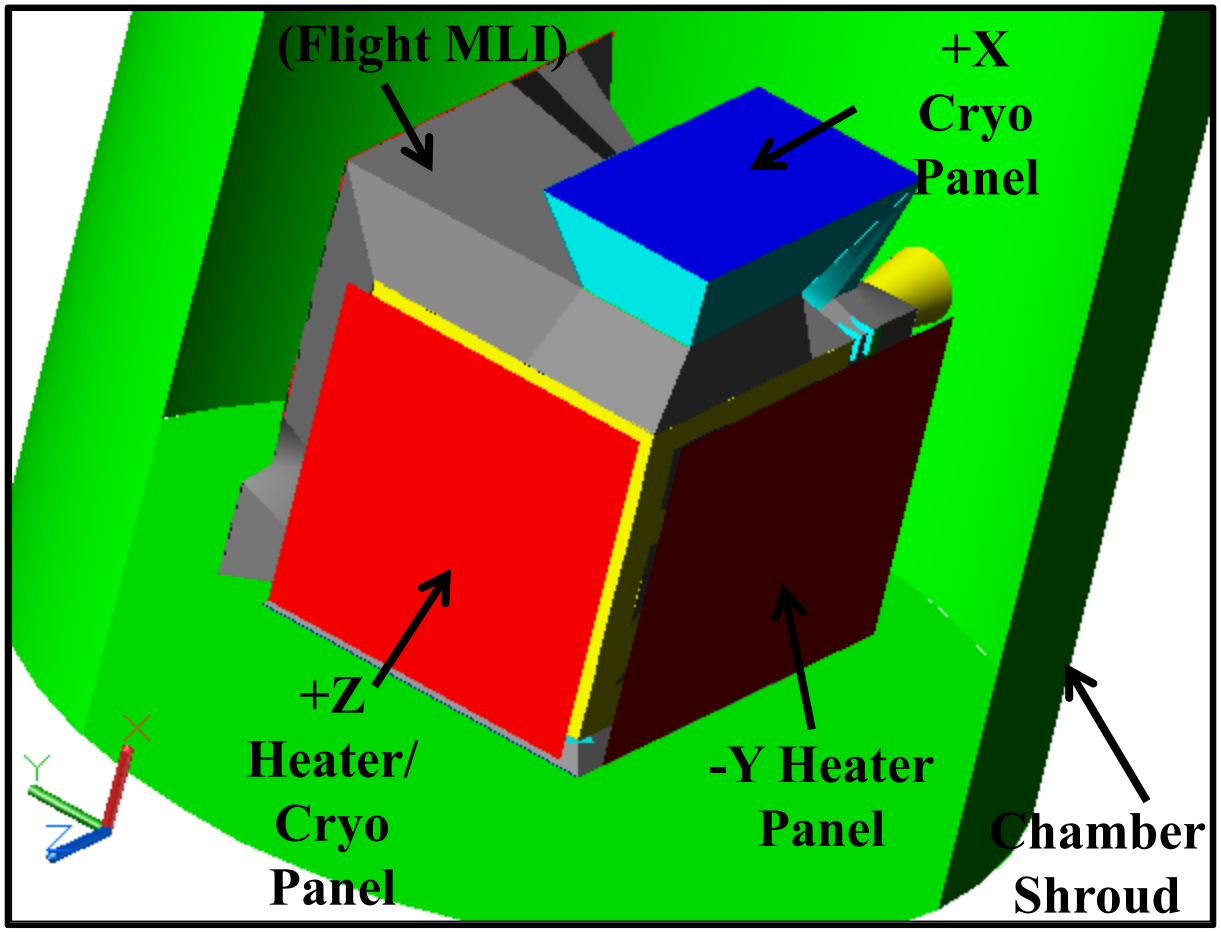

Thermal Desktop Model of TVac Setup

Test Design Constraint: Avoid –Z Side, Goal: 3 Panels

Temperature and Power Comparison

- Evaluation of Test Design:
  - Temperature
    - **Most** components are within 2˚ C of flight predictions
    - Compromise necessary on Liquid Line
  - Heater Power
    - **Most** components are 10% or 0.5W of flight predictions

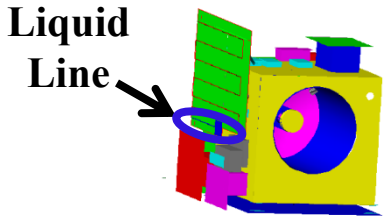

Legend:

+X Cryo Panel
-Y Heater Panel
+Z Heater Panel
Shroud

	HB00		HB70		CB90		CB90 Survival	
	Temperature Difference (°C)	Heater Power Difference (%)	Temperature Difference (°C)	Heater Power Difference (%)	Temperature Difference (°C)	Heater Power Difference (%)	Temperature Difference (°C)	Heater Power Difference (%)
PDU I/F	0.3	0%	-0.7	0%	0.7	0%	0.0	1%
LRS Elec I/F	1.4	0%	1.7	0%	1.7	0%	0.1	-3%
LRS Opt I/F	-0.1	13%, 0.3 W	0.0	-7%	0.0	-5%	-0.1	0%
Beam Expander	-0.7	0%	-0.4	0%	-1.2	0%	-1.4	4%
Telescope Primary	0.7	0%	0.6	0%	0.1	-12%, -0.2W	1.1	0%
MEB I/F	1.1	0%	1.9	0%	1.8	0%	0.2	-6%
DAA Elec I/F	0.8	0%	1.3	0%	1.1	0%	-0.1	-5%
DAA Optics I/F	-1.6	0%	-0.3	0%	0.0	0%	0.0	-5%
LHP Liquid Line	-16.8	0%	-7.9	0%	1.2	32%	0.1	6%

Summary of Thermal Panel Setpoints

- Results
  - Setpoints will be used in Thermal Vacuum Test Plan
  - **Realized that +Z Panel must be a Cryo Panel**

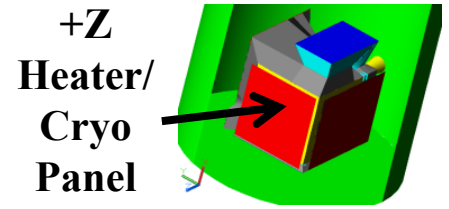

	HB00			HB70			CB90			CB90 Survival		
	Flight Sink (°C)	Test Sink (°C)	Test Power (W)	Flight Sink (°C)	Test Sink (°C)	Test Power (W)	Flight Sink (°C)	Test Sink (°C)	Test Power (W)	Flight Sink (°C)	Test Sink (°C)	Test Power (W)
+X Cryo Panel	-47	-76	-92	-63	-108	-97	-101	-138	-83	-94	-119	-59
-Y Heater Panel	-74	110	510	26	135	676	-28	50	259	-84	60	302
+Z Heater Panel	7	32	101	17	23	59	-28	-28	10	-80	-60	-26
Shroud	-78	-100	n/a	-84	-101	n/a	-97	-115	n/a	-85	-105	n/a

- Observations
  - -Y Heater Panel is significantly warmer than flight sink
    - Due to initial testing constraint (avoid –Z), the –Y panel is used to drive optics warm
    - Effects in HB00: Structure 8° C warmer on –Y side, Optical Bench 1° C warmer on –Y side
  - Mitigation Possibilities (Future Work)
    - Split –Y heater panel into two panels, adding an extra zone
    - Place a heater panel on –Z side
    - If testing constraints do not yield, continue with current test design

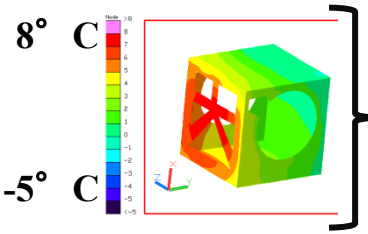

Structure Temp Difference: Test Minus Flight

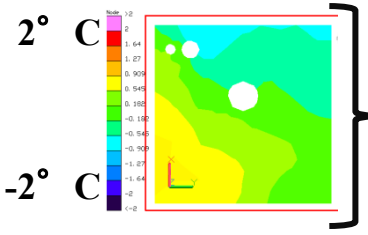

Optical Bench Temp Difference: Test Minus Flight

Overview of Optics and STOP Analysis

- Location of alignment-sensitive optics:
  - Optical Bench, -Z side of ATLAS

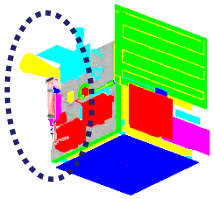

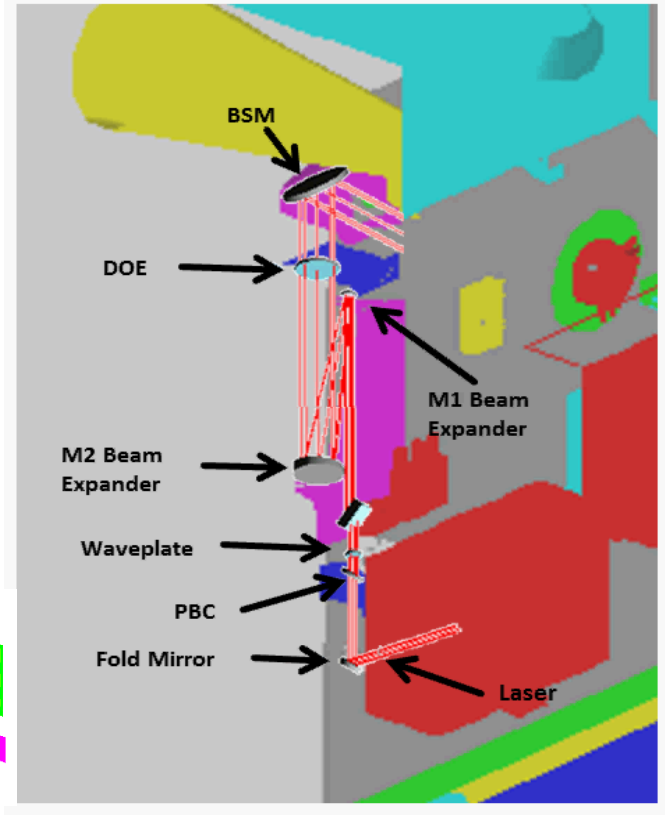

Transmit Beam Path

- Overview of STOP analysis
  - Generate temperatures
  - Map TD to FEM
  - **Validate mapping**
  - Generate displacements
  - Generate LOS errors
  - **Compare results to requirements**

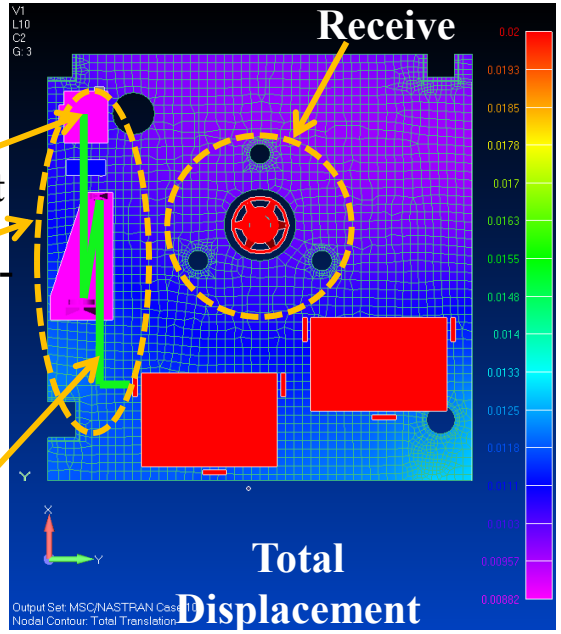

Mapping Verification: HB70 Flight Case

NASTRAN TEMPERATURE PLOT

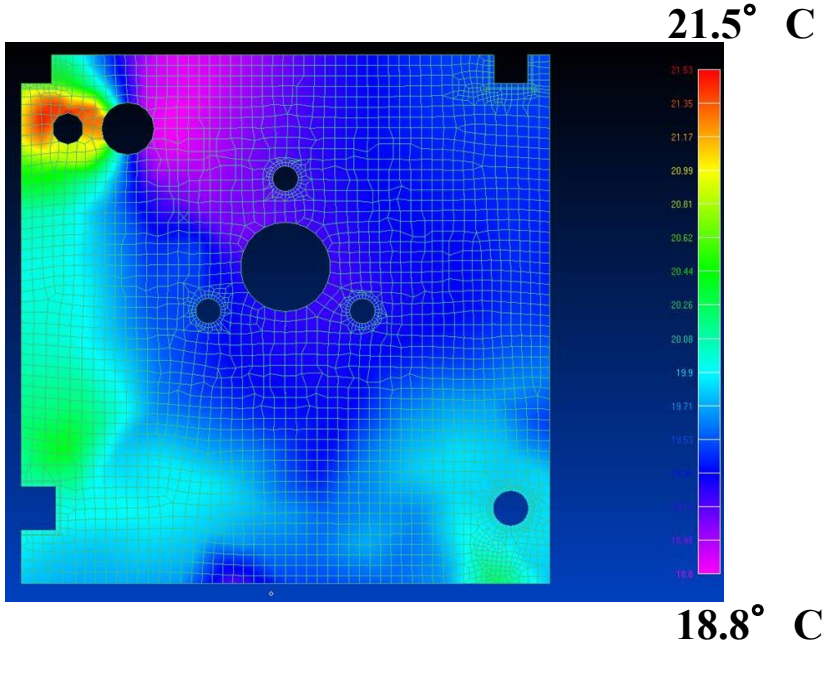

THERMAL DESKTOP TEMPERATURE PLOT

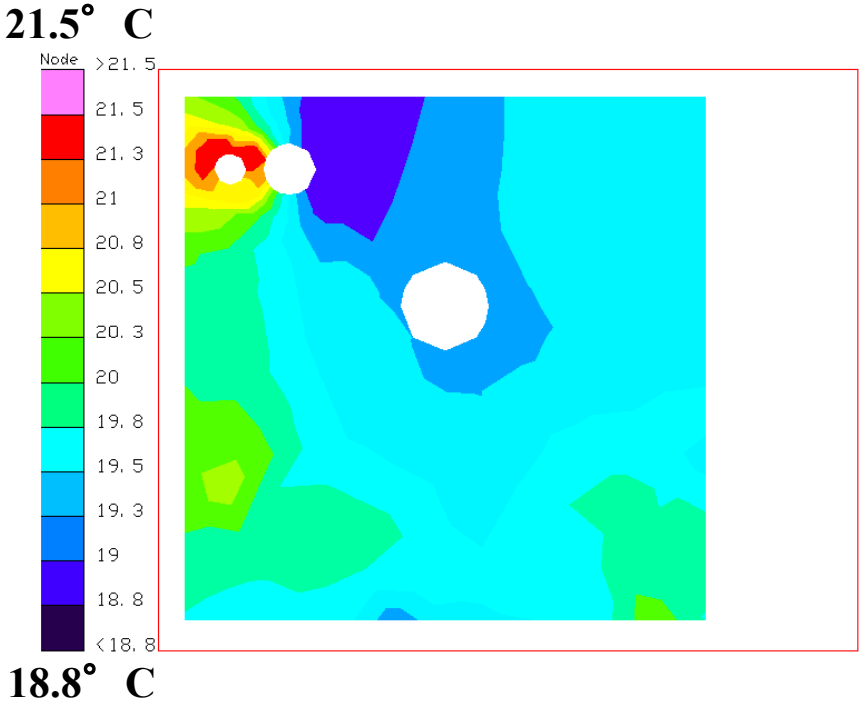

- **Reasonability check for mapping process:**
  - **NASTRAN and Thermal Desktop (TD) temperatures for OB are in agreement**
  - **Implies the TD nodes have been mapped to NASTRAN nodes successfully**

HB70 LOS Results: Error Within Requirements

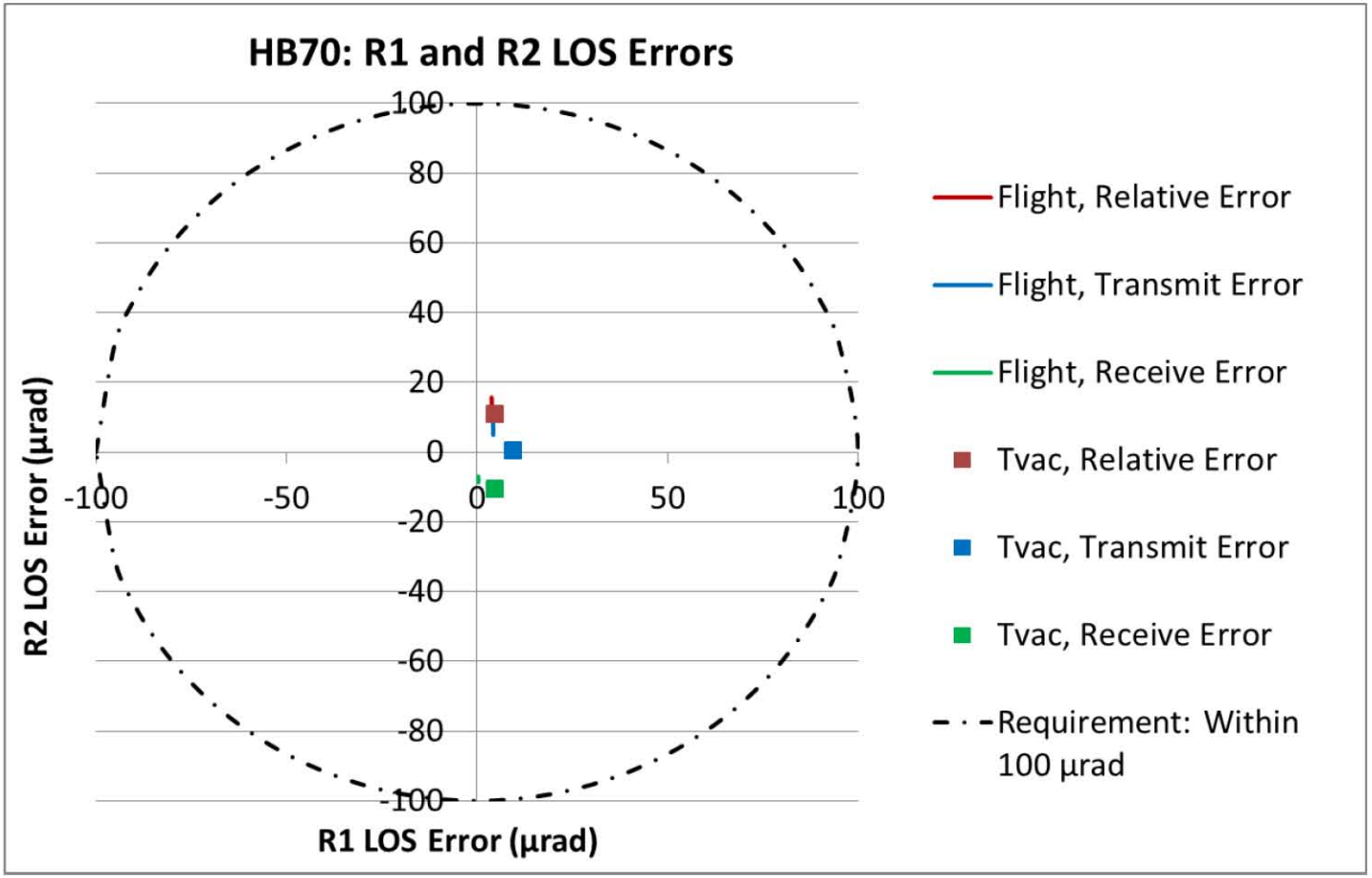

- Note: Requirement for max allowable LOS error is 100 urad
- Results indicate predicted LOS errors meet this requirement

HB70 LOS Results

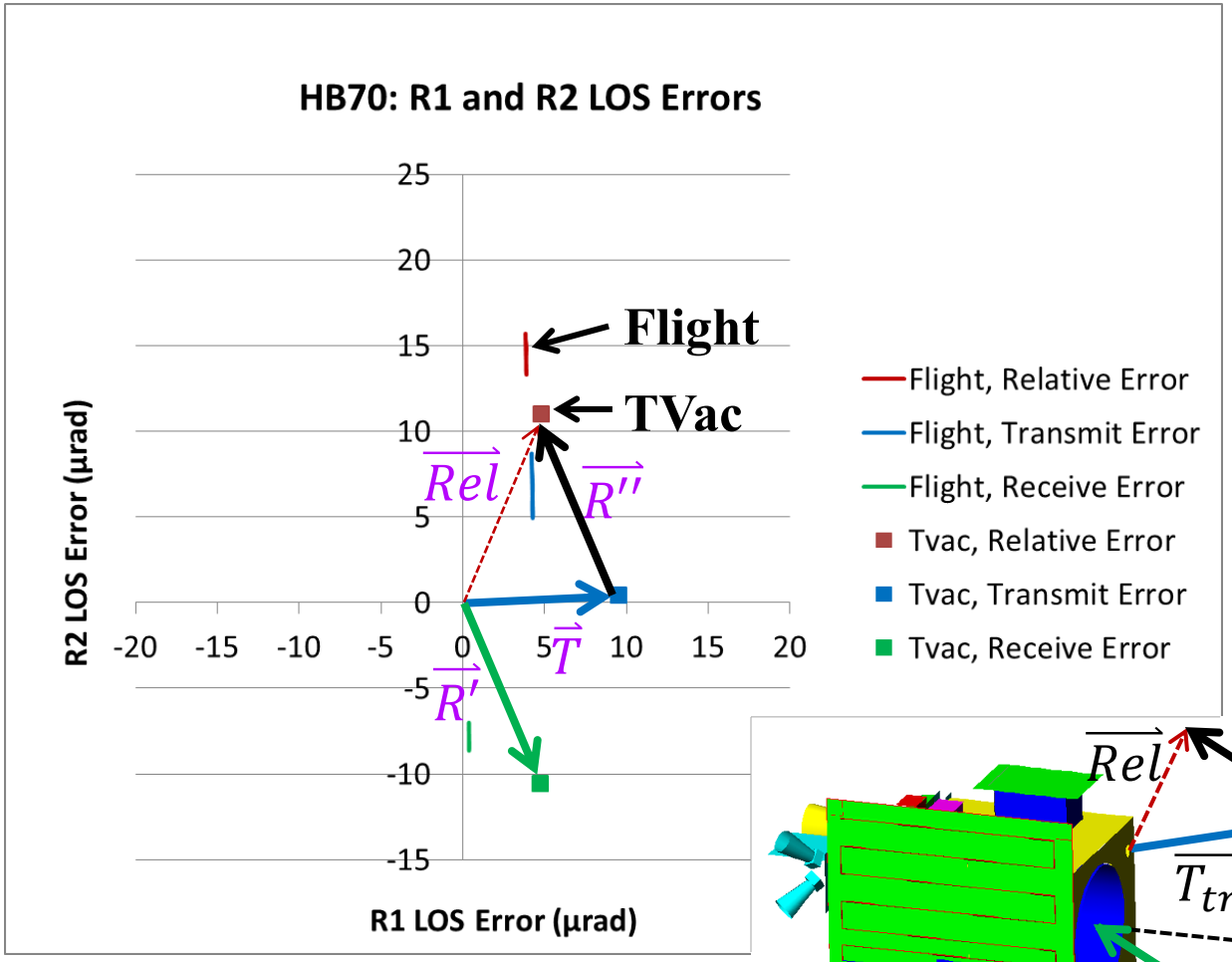

Questions Investigated:

- **A) Why are test and flight predictions not aligned?**
- **B) Which part of the orbit causes the most distortion?**

- **Vector subtraction used to calculate relative (total) pointing error**

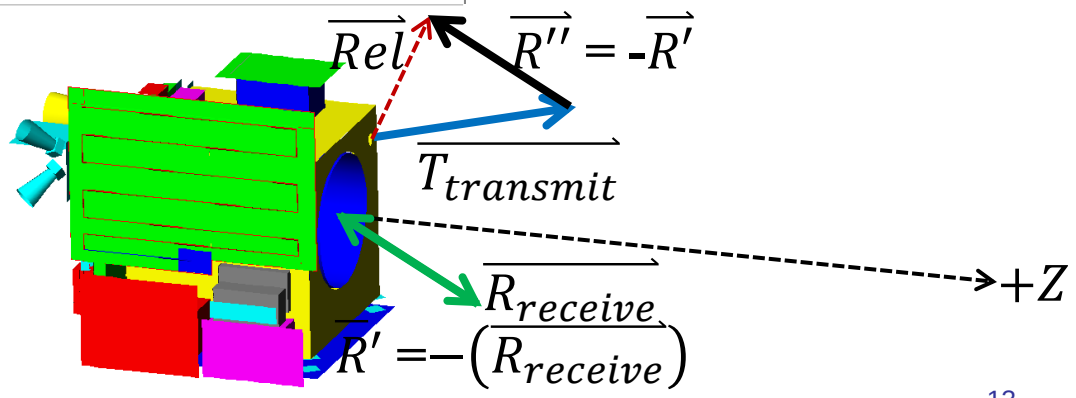

Question A: Test to Flight Comparison

Flight:

Test:

Flight:
OB Temperature

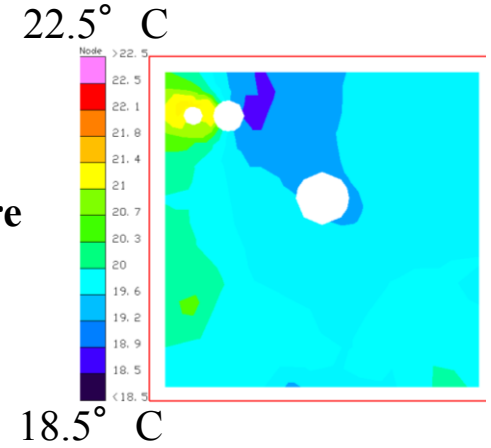

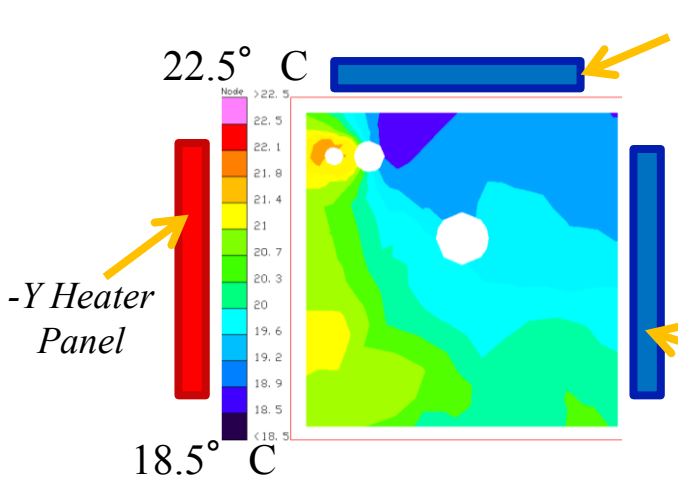

Test:
OB Temperature

Flight:
Total Displacement of OB

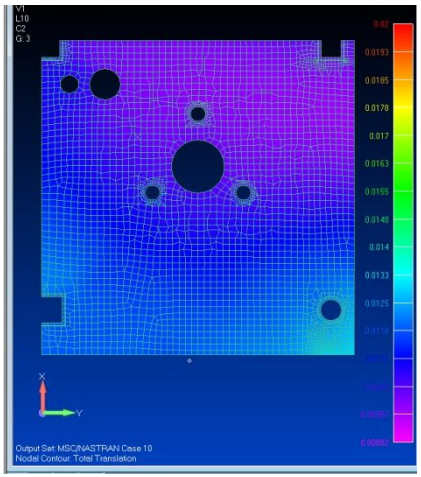

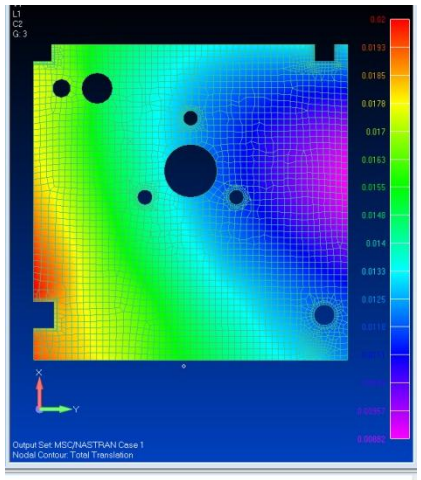

Test:
Total Displacement of OB

Therefore, it is reasonable that Flight LOS will <u>differ</u> slightly from TVac

Question B: Orbit Variation Contributes to LOS Increase

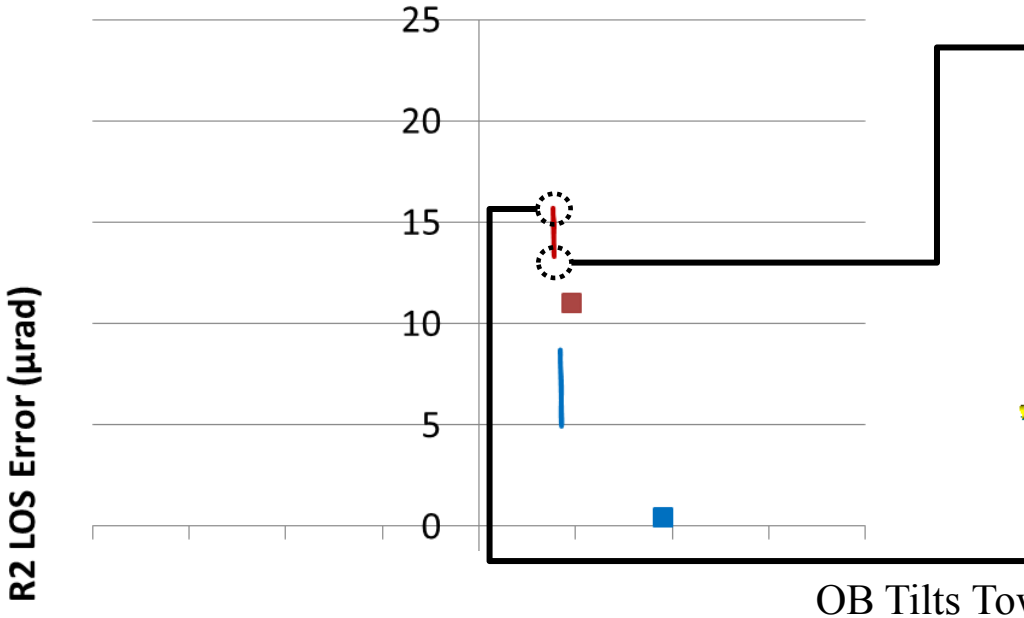

OB Tilts Away from Sun (colder)

22° C

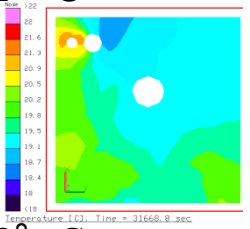

18° C

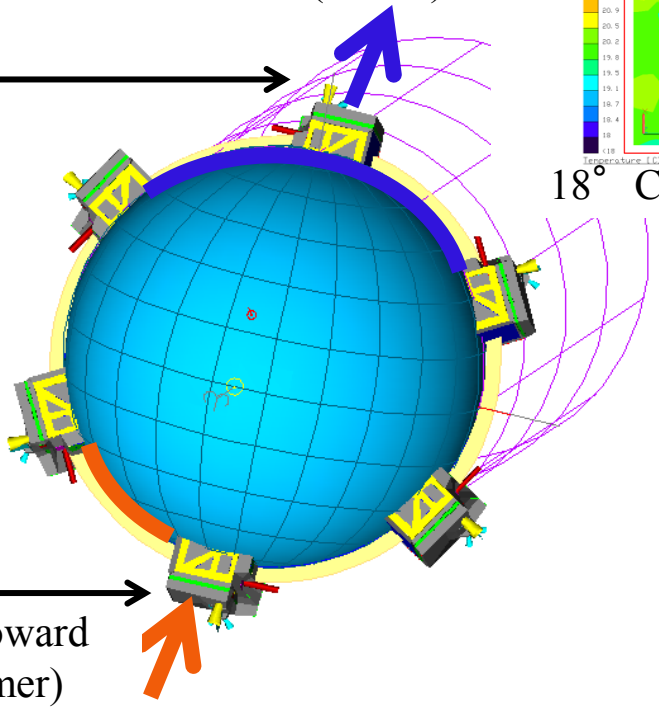

OB Tilts Toward Sun (warmer)

22° C

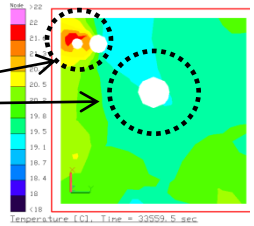

18° C

Increased temperature near beam transmit and receive regions (**may lead to greater pointing error**)

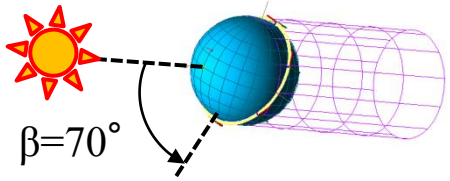

Conclusions

- Thermal Vacuum Test Design
  - Determined **temperature setpoints and power** required for thermal panels
  - Verified **temperature predictions** of instrument match flight
  - Verified heater **power predictions** of instrument match flight
  - Verified that TVac **heat flows** are similar to flight heat flows

- STOP Analysis
  - Verified that ATLAS will perform **within pointing requirements** in test, error is well within 100 μrad
  - Verified that TVac LOS predictions are **close to flight predictions**, within 15 μrad

Future Work

- Test Design
  - Systems-level decision on –Y heater panel
  - Develop specifications for heater and cryo panels
  - Obtain hardware: build or locate existing panels for test

- STOP Analysis
  - Include s/c and s/c interface plate in structural model
  - Include detailed thermal analysis of optics

Acknowledgements

- David Steinfeld
- Matt Garrison
- Deepak Patel
- Sheila Wall
- Laurie Seide
- Lun Xie
- Hume Peabody
- Kan Yang
- John Hawk
- Juan Rodriguez-Ruiz
- Richard D'Antonio
- Luis Ramos-Izquierdo
- Dan Nguyen
- Wes Ousley
- Carol Mosier
- Justin Brannan
- Kevin Fisher
- Ron Jones
- Eduardo Rodriguez
- Rivers Lamb
- Elaine Lin
- Brian Simpson
- Joe Bonafede
- Sassan Yerushalmi

Thank you for your attention. Questions?

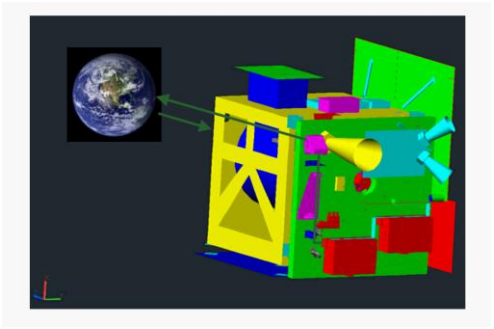

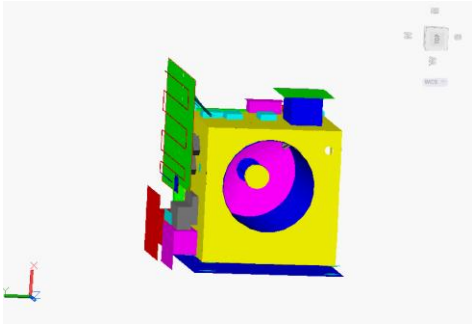

AUDIENCE HANDOUTS

Glossary of Acronyms

- AMCS: Alignment Monitoring and Control System
- ATLAS: Advanced Topographic Laser Altimeter System
- BDF: Bulk Data File
- BSM: Beam Steering Mechanism
- CB: Cold Beta
- DAA: Detector Array Assembly
- DOE: Diffractive Optical Element
- FOV: Field of View
- GLAS: Geoscience Laser Altimeter System
- GSE: Ground Support Equipment
- GSFC: Goddard Space Flight Center
- HB: Hot Beta
- ICESat-2: Ice, Cloud, and land Elevation Satellite-2
- I/F: Interface
- IR: Infrared
- LHP: Loop Heat Pipe
- LOLA: Lunar Orbiter Laser Altimeter
- LOS: Line of Sight
- LRS: Laser Reference System
- LSA: Laser Sampling Assembly
- MEB: Main Electronics Box
- MLA: Mercury Laser Altimeter
- MLI: Multi-Layer Insulation
- MOLA: Mars Orbiter Laser Altimeter
- NASTRAN: NASA Structural Analysis
- OB: Optical Bench
- PBC: Polarizing Beam Combiner
- PDU: Power Distribution Unit
- PIP: Professional Intern Program
- PRF: Pulse Repetition Frequency
- S/C: Spacecraft
- SCIF: Spacecraft Interface
- STOP: Structural Thermal Optical Performance analysis
- TD: Thermal Desktop
- TVac: Thermal vacuum

ATLAS Diagrams for Reference

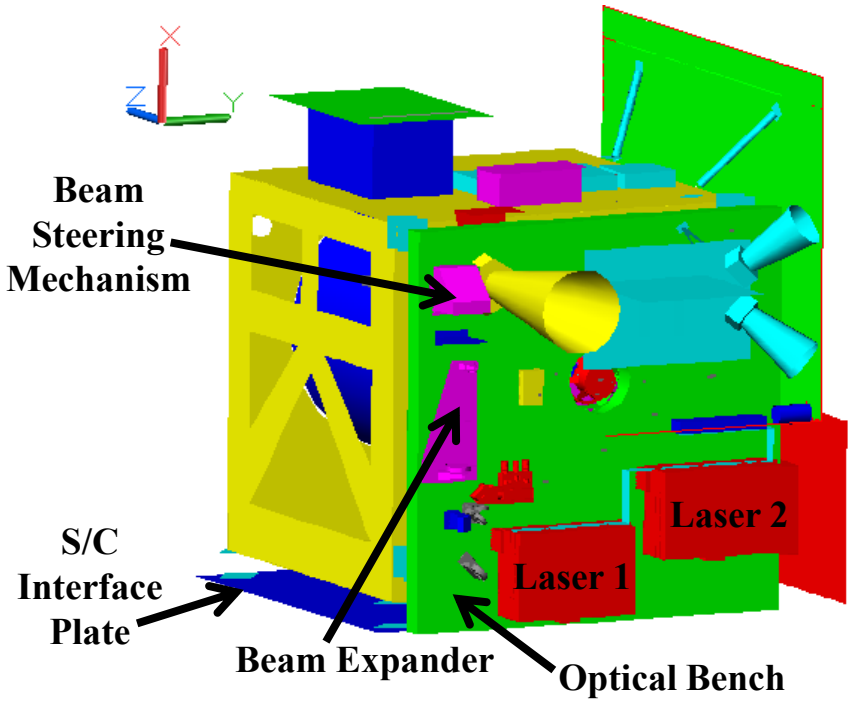

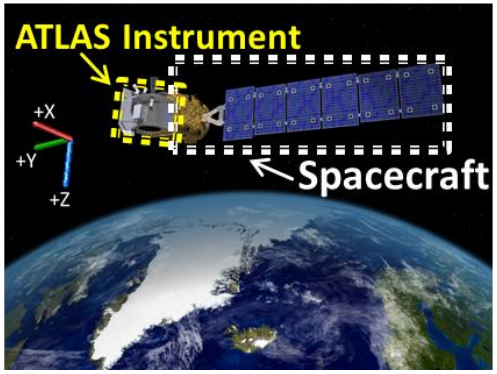

Axes and Rotations for Reference:

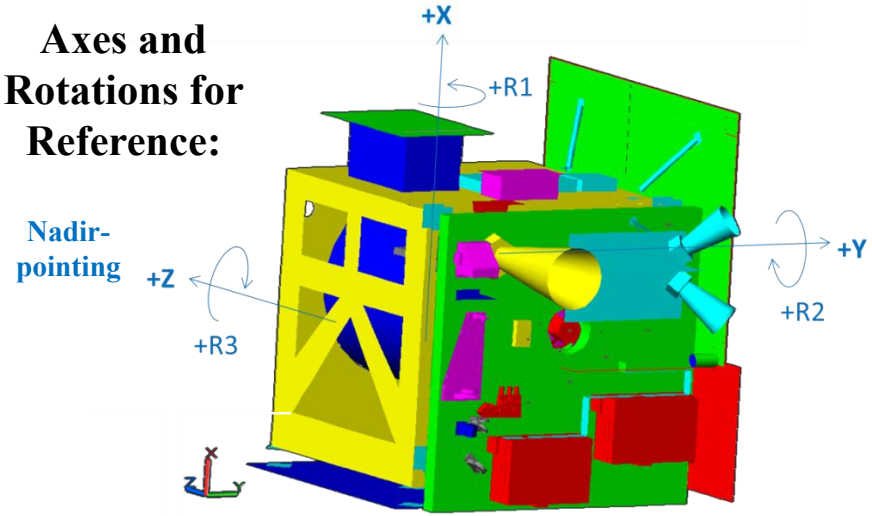

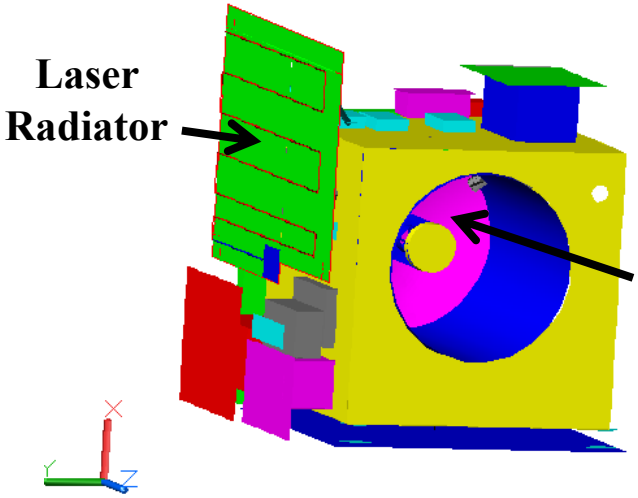

BACKUP SLIDES

Sink Temperature Calculations, Preliminary Estimates

Goals for each component:
- +/- 2°C of flight
- +/- 0.5W or 10% of flight
- Note: Compromise may be necessary

$$Q_{radiation} = A * e * \sigma * \left(T^4 - T_s{}^4\right)$$

- **Sink Temperature Calculation Based on Temperature:**
  - **Heaters are off, box is turned on, constant dissipation**
  - **Last iteration = subscript 1; Next iteration = subscript 2**

$$Q_{1,test} = Q_{2,flight}$$

$$\cancel{A_{component} * e_{component} * \sigma *} \left(T_{1,test}{}^4 - T_{sink1}{}^4\right) = \cancel{A_{component} * e_{component} * \sigma *} \left(T_{2,flight}{}^4 - T_{sink2}{}^4\right)$$

$$T_{sink2,\,by\,temp} = \sqrt[4]{\left(T_{2,flight}\right)^4 - \left(T_{1,test}\right)^4 + \left(T_{sink1}\right)^4}$$

- Sink Temperature Calculation Based on **Power**:
  - Heater power on, positive control, constant temperature
  - Use ratio of heater powers to calculate new sink

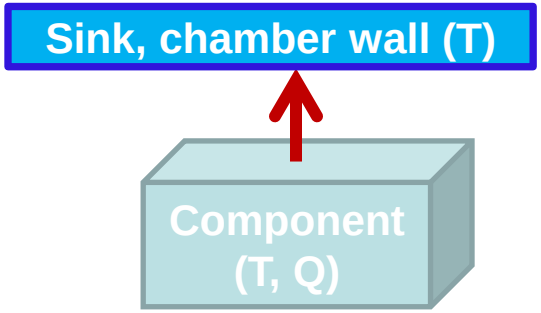

$$\frac{Q_{2,\,flight}}{Q_{1,\,test}} = \frac{\left(T_{flight}{}^4 - T_{sink2}{}^4\right)}{\left(T_{flight}{}^4 - T_{sink1}{}^4\right)}$$

$$T_{sink2,\ by\ power} = \sqrt[4]{\left(T_{flight}\right)^4 + \left(\frac{Q_{2,\,flight}}{Q_{1,test}}\right)\left[\left(T_{sink1}\right)^4 - \left(T_{flight}\right)^4\right]}$$

HB70 Temperature Difference Comparison Between Flight and Test

- **Temperature Comparison:**
  - **Left Edge (-Y)**
    - Slightly warmer in tvac than flight
    - Proximity to tvac heater plate used to drive optics
  - **Top Edge (+X)**
    - Slightly cooler than flight
    - Proximity to tvac cryo plate used to drive electronics
  - **Overall**
    - OB tvac temperatures are within +/- 2°C of flight predictions (for all cases)
    - This is within testing tolerances

Test Minus Flight:
Map of Temperature Difference

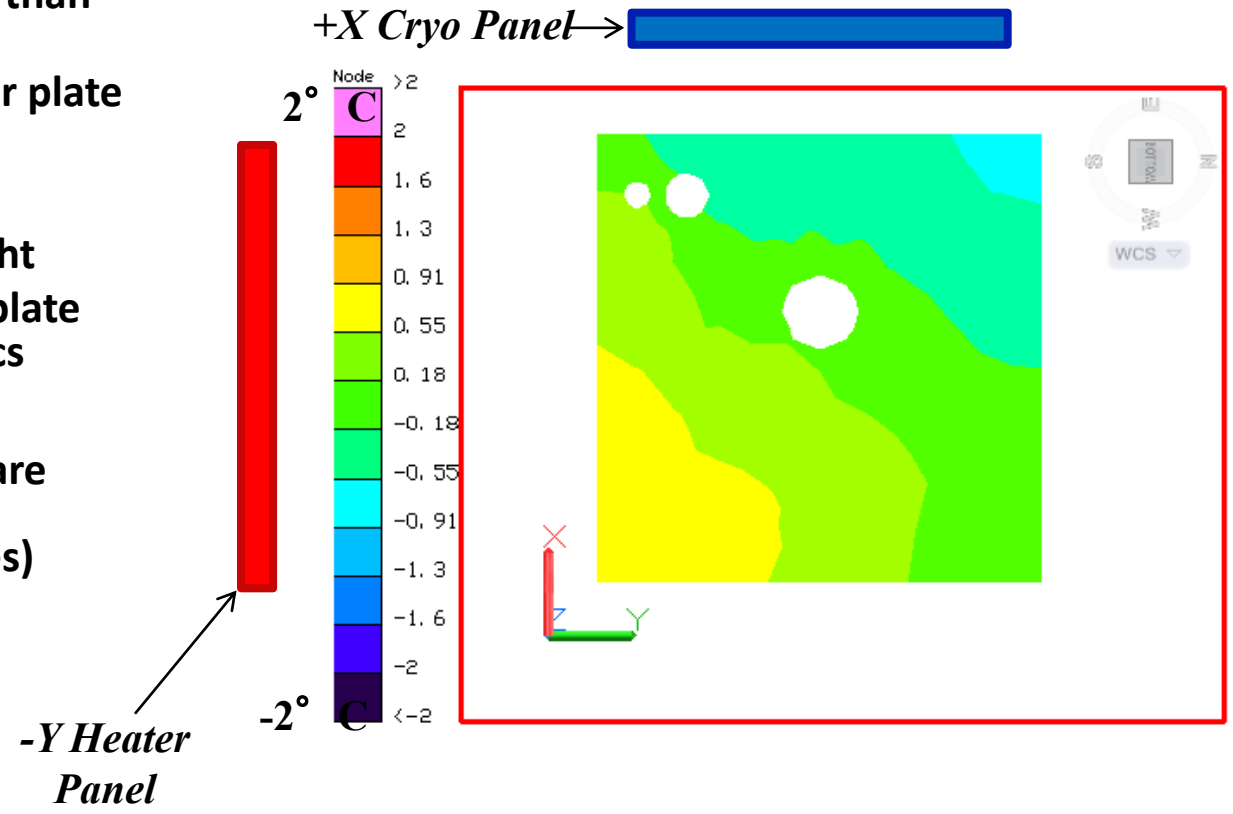

HB70 Delta T
(chamber minus flight)

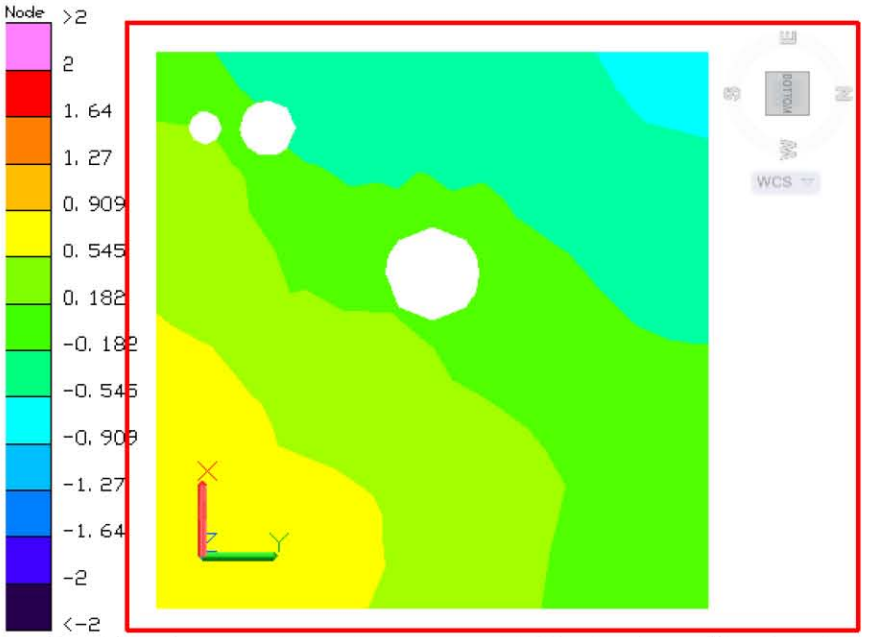

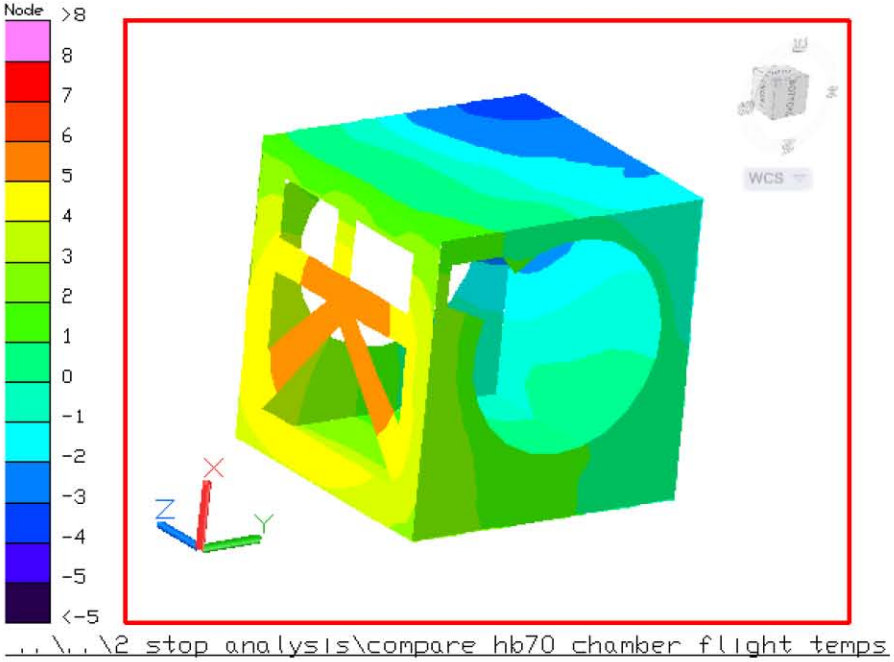

CB90 Delta T
(chamber minus flight)

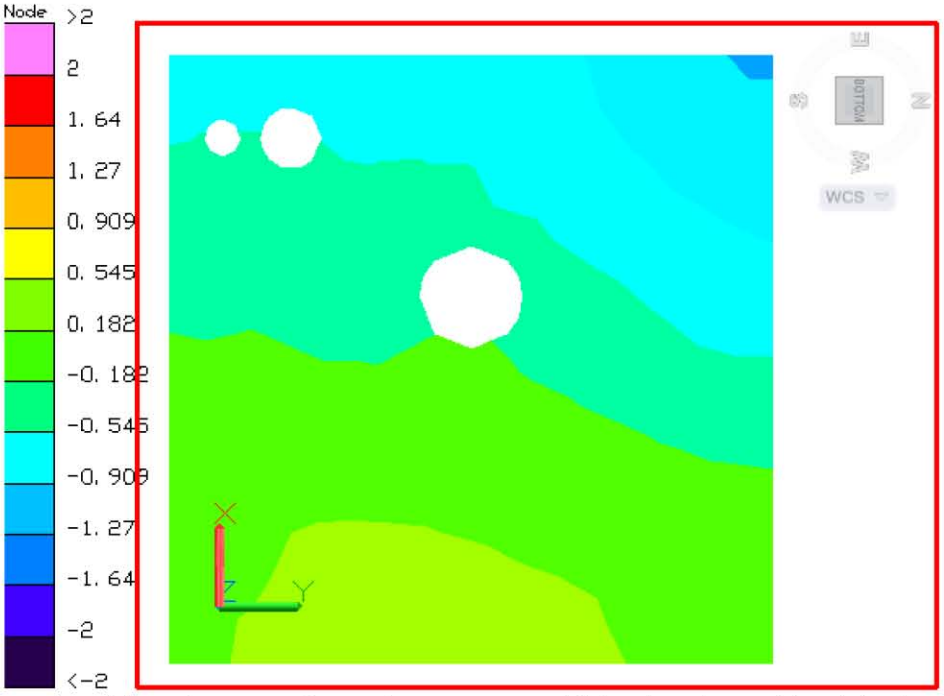

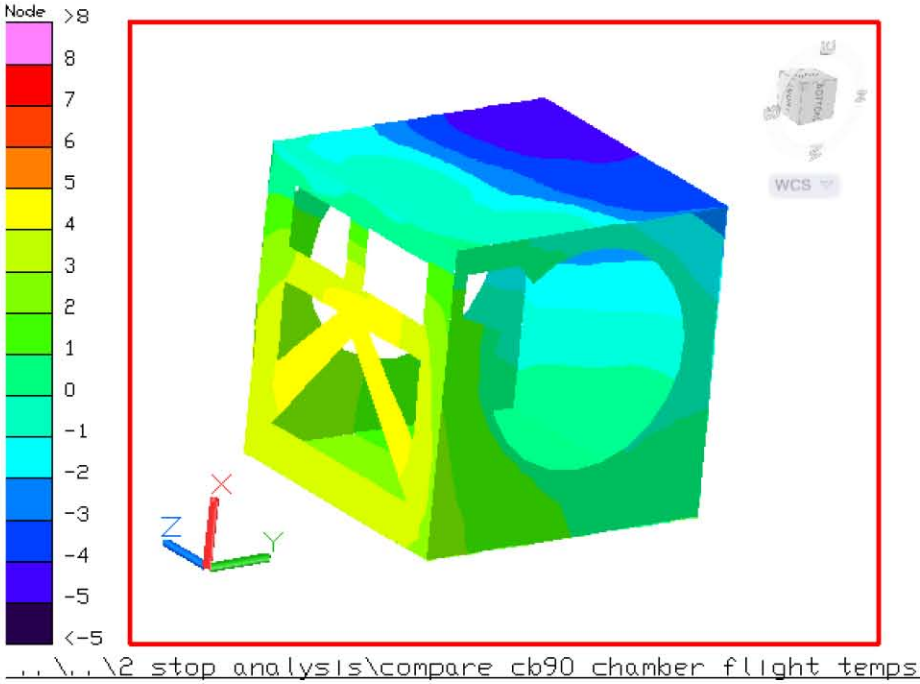

CB90 and HB00 LOS Results: Error Within Requirements

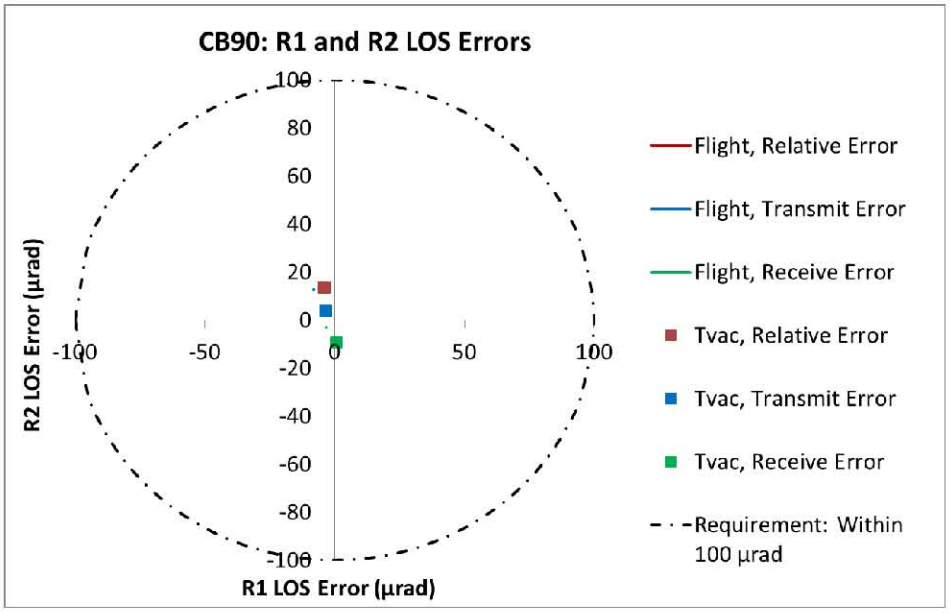

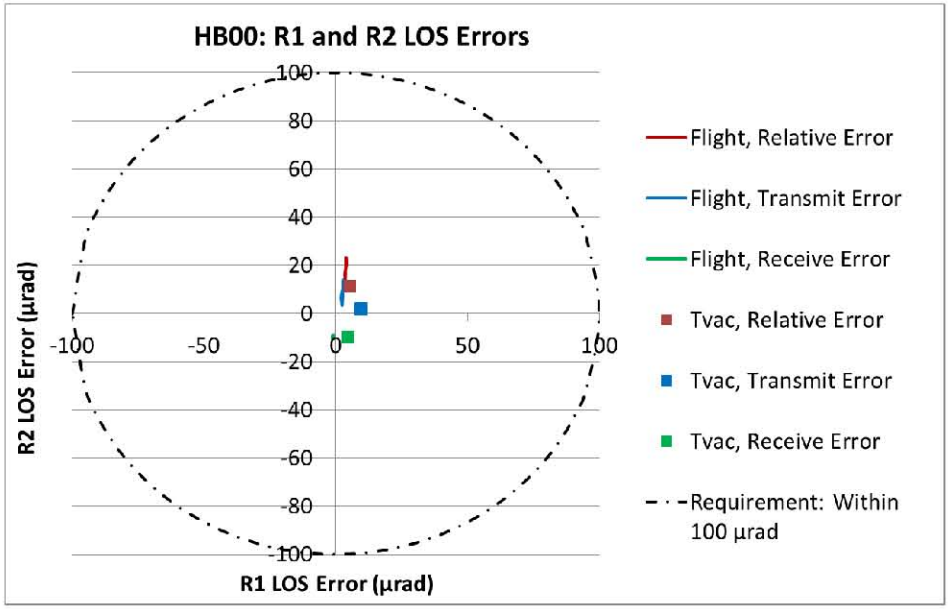

LOS Results: HB70 Case

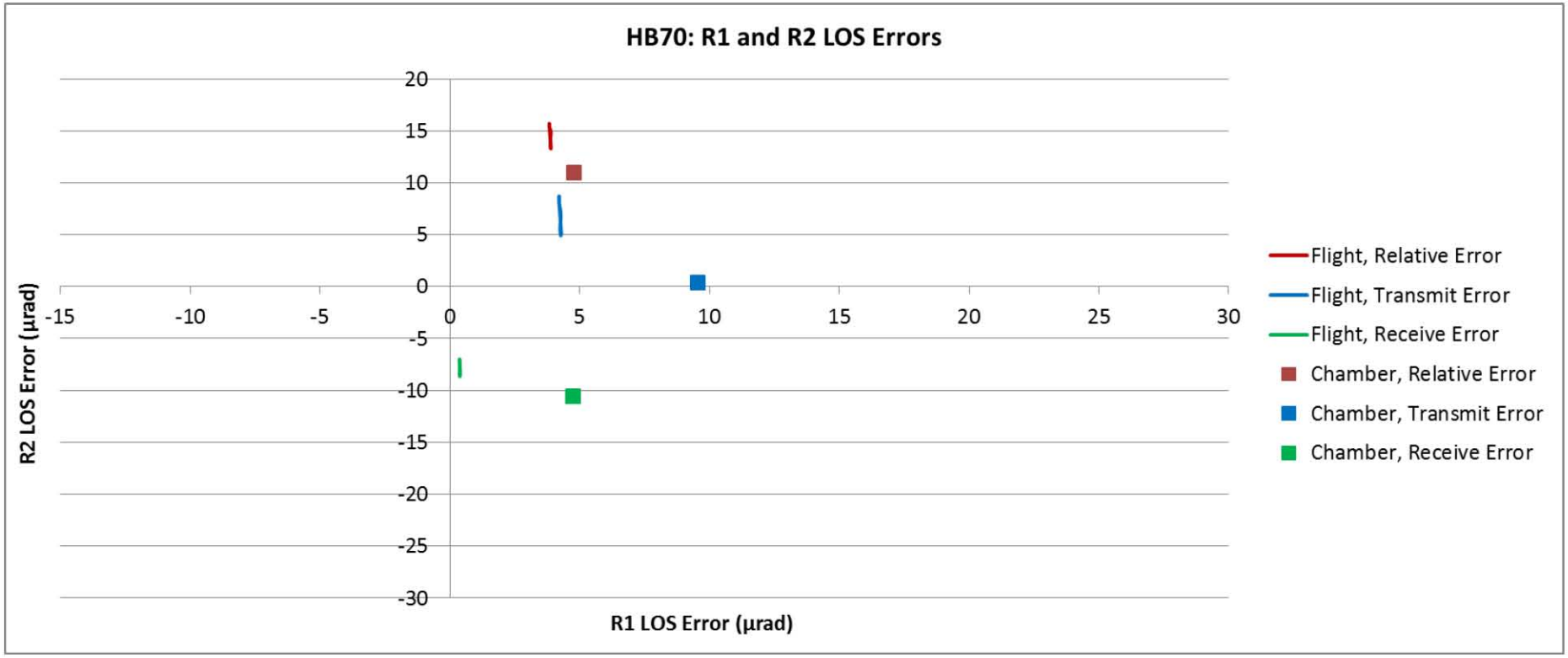

LOS Results: CB90

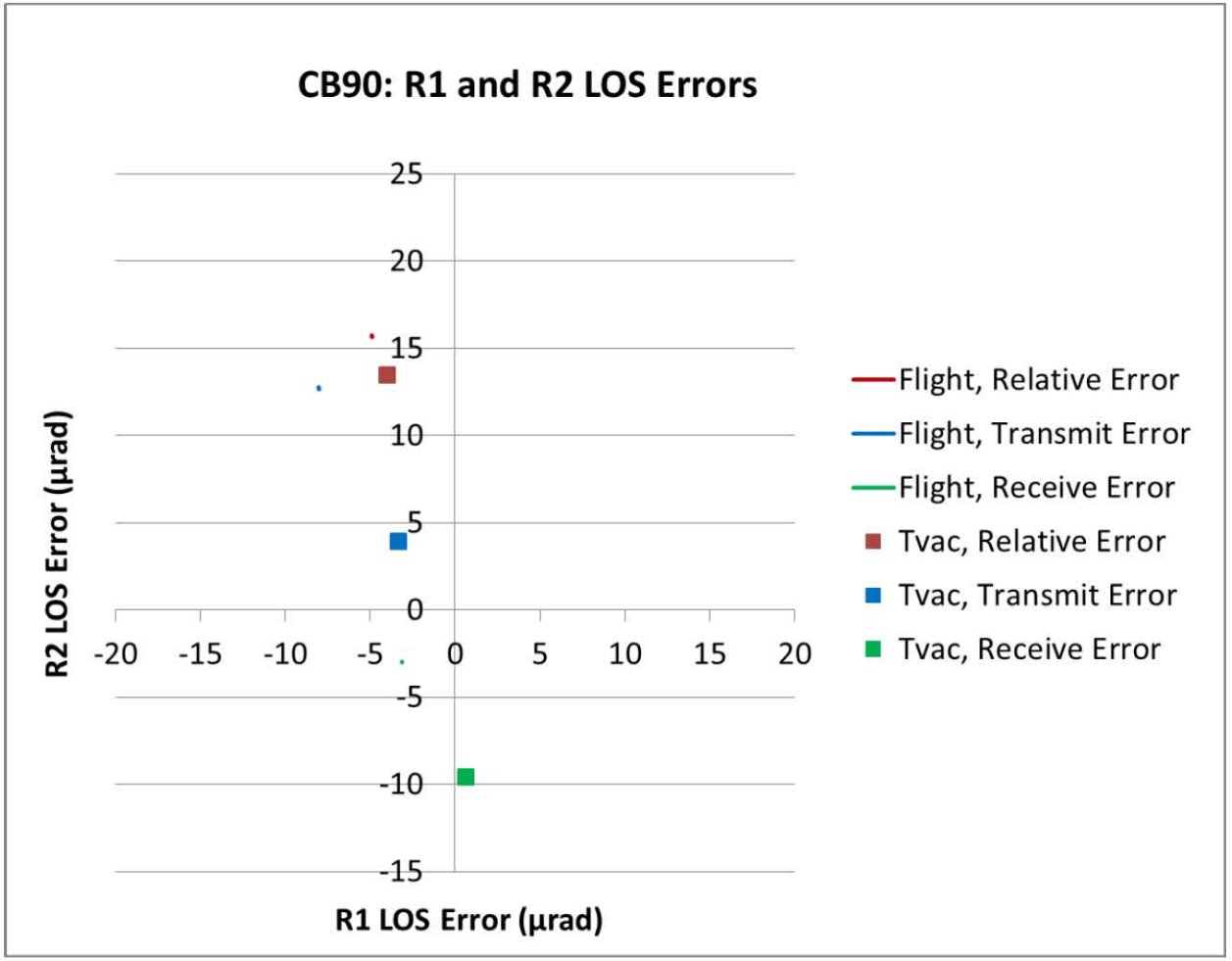

THERMAL AND ALIGNMENT ANALYSIS OF THE INSTRUMENT-LEVEL ATLAS THERMAL VACUUM TEST

Heather Bradshaw

Thermal Engineering Branch, Code 545
NASA Goddard Space Flight Center

ABSTRACT

This paper describes the thermal analysis and test design performed in preparation for the ATLAS thermal vacuum test. NASA's Advanced Topographic Laser Altimeter System (ATLAS) will be flown as the sole instrument aboard the Ice, Cloud, and land Elevation Satellite-2 (ICESat-2). It will be used to take measurements of topography and ice thickness for Arctic and Antarctic regions, providing crucial data used to predict future changes in worldwide sea levels. Due to the precise measurements ATLAS is taking, the laser altimeter has very tight pointing requirements. Therefore, the instrument is very sensitive to temperature-induced thermal distortions. For this reason, it is necessary to perform a Structural, Thermal, Optical Performance (STOP) analysis not only for flight, but also to ensure performance requirements can be operationally met during instrument-level thermal vacuum testing. This paper describes the thermal model created for the chamber setup, which was used to generate inputs for the environmental STOP analysis. This paper also presents the results of the STOP analysis, which indicate that the test predictions adequately replicate the thermal distortions predicted for flight. This is a new application of an existing process, as STOP analyses are generally performed to predict flight behavior only. Another novel aspect of this test is that it presents the opportunity to verify pointing results of a STOP model, which is not generally done. It is possible in this case, however, because the actual pointing will be measured using flight hardware during thermal vacuum testing and can be compared to STOP predictions.

INTRODUCTION

The Ice, Cloud, and land Elevation Satellite-2 (ICESat-2) is studying changes in levels of ice and vegetation on the Earth, collecting data that will inform scientists' understanding of climate change on the planet. The science objectives of the mission include: (a) studying land ice, especially in the polar regions, and quantifying its effects on sea-level change, (b) estimating the thickness of sea ice and examining its effects on energy exchanges with the atmosphere, and (c) measuring canopy height of vegetation in order to estimate biomass change of the planet [1]. The spacecraft will be in a near-circular, near-polar orbit at an altitude of 481km. Visualizations of ICESat-2 in space are shown in Figure 1. The mission duration is planned for three years (with propellant for seven years), and the launch date is scheduled for 2016 [2].

ICESat-2 is a single-instrument spacecraft, with the Advanced Topographic Laser Altimeter System (ATLAS) serving as the sole instrument.

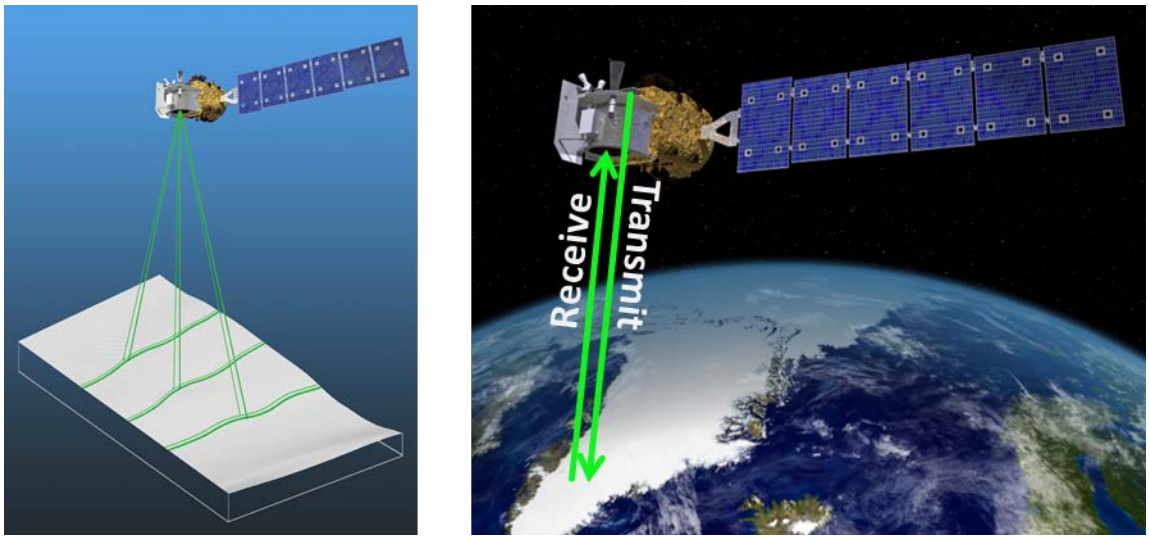

Figure 1. Visualizations of ICESat-2 in space [1, 2].

Laser altimetry is used to measure the topography of ice sheets and vegetation for the ICESat-2 mission. Laser altimeter systems similar to this have been used before, on instruments such as MOLA, LOLA, and GLAS. However, compared to these and other laser altimeters that Goddard Space Flight Center (GSFC) has built in the past, the ATLAS instrument has the following unique challenges: it has the smallest receiver field of view, the smallest transmitted beam, and the smallest alignment margin that GSFC has ever attempted, as illustrated in Figure 2 [3]. As a note, a full list of acronyms and their meanings is provided in Appendix A. Also, additional reference diagrams of the ATLAS instrument, with major components labeled, are provided in Appendix B.

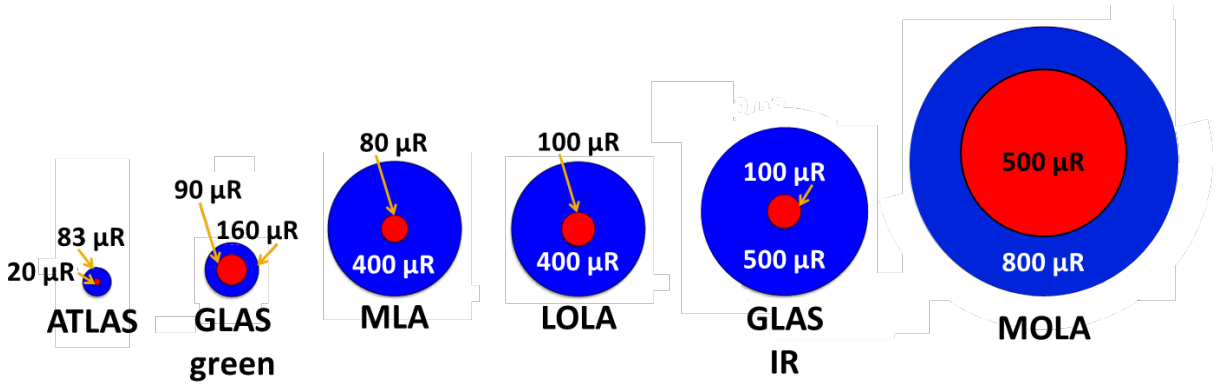

Figure 2. Comparison between laser beam (red) and receiver field of view (blue) of previous laser altimeters [3].

Because the instrument has unusually tight pointing requirements, ATLAS has an active alignment system onboard, called the Alignment Monitoring Control System (AMCS), which must be demonstrated to work in the thermal vacuum test environment. Most instruments do not have an active alignment system - as such, there is not a driving need to perform a Structural, Thermal, Optical Performance (STOP) analysis for thermal vacuum (TVac) testing. Therefore, the STOP analysis is usually performed only for flight. However, for the ATLAS instrument, a STOP analysis was performed for both test and flight predictions, because it is critical to simulate flight-like optical pointing during TVac. It is also critical to verify that the Line of Sight (LOS) pointing error will be within requirements while in the chamber, so that functionality of the AMCS can be verified during environmental testing, which further adds to the motivation for performing the STOP analysis.

The ATLAS thermal vacuum test is currently scheduled for 2015. The overall objectives of the test are: (a) achieve thermal balance at four bounding cases, to collect data for use in correlating the thermal model, (b) perform thermal cycling to qualify flight hardware and verify instrument performance, (c) bake out flight hardware and verify that outgassing requirements are met, and (d) verify that the AMCS is able to correct for temperature-induced misalignments of the laser's transmitted and received beams [5].

This paper describes the design and analysis of the chamber setup that will be used to simulate flight-like temperature, heater power, and Line of Sight (LOS) pointing conditions during TVac. The first portion of the paper describes the development of the chamber model, including the process used to arrive at temperature setpoints of the thermal panels, which will be used as inputs to the ATLAS thermal vacuum test plan. The latter portion of this paper describes the results of the unique STOP analysis that was performed in preparation for this TVac test.

DESIGN OF THERMAL VACUUM SETUP: SETPOINTS OF HEATER PANELS AND CRYO PANELS

The goal in designing the chamber setup is to arrange the thermal vacuum environment in such a way that it simulates the effects of the flight environment as closely as possible.

In order to accomplish this, first, a thermal model was built using Thermal Desktop, to represent the thermal vacuum chamber environment, and the existing ATLAS instrument model was inserted into this model for analysis of the instrument-level thermal vacuum test. To simulate flight-like conditions inside the chamber, several thermal control surfaces were used. They were placed at the locations shown in Figure 3. These control surfaces included the chamber shroud, as well as a heater panel on the –Y side of the instrument, a cryo panel on the +Z side of the instrument, and another a cryo panel on the +X side. The fifth thermal control surface is the Spacecraft Control Interface Plate (SCIF), located on the –X side; this is not visible in Figure 3, but is located underneath the instrument on the –X side. The outcome of this chamber design analysis included a determination of the location and temperature setpoints needed for each of these thermal control surfaces inside the chamber. In order to determine

whether the test setup simulated flight conditions well, the following results were compared between test and flight: instrument temperatures, heater powers, and line of sight pointing errors. The design approach was to develop a test setup that simulated the first two of those very well, and then to analyze the line of sight pointing errors that would occur given this test setup, and verify whether the instrument would meet pointing requirements in this setup.

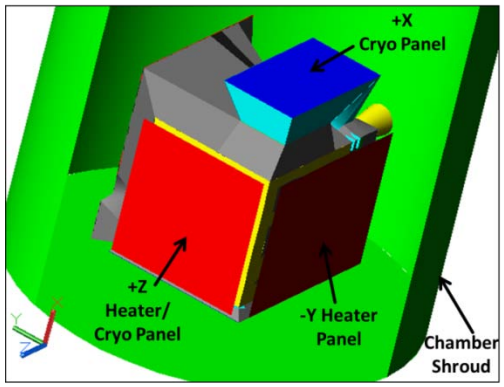

Figure 3. Location of four thermal control surfaces in test.

The cases that were selected for this analysis were the four bounding orbit cases that will be used as thermal balance points during the thermal vacuum test: Hot Beta 0°, Hot Beta 70°, Cold Beta 90°, and Cold Beta 90° Survival. As a note, the Cold Beta 90° Survival case places the instrument in a solar-inertial configuration (with sun on –Y side), while the Cold Beta 90° operational case is nadir-pointing. Images of the orbit beta angles are shown in Figure 4. As a note, Beta angle (β) refers to the angle between the solar vector and the orbit plane.

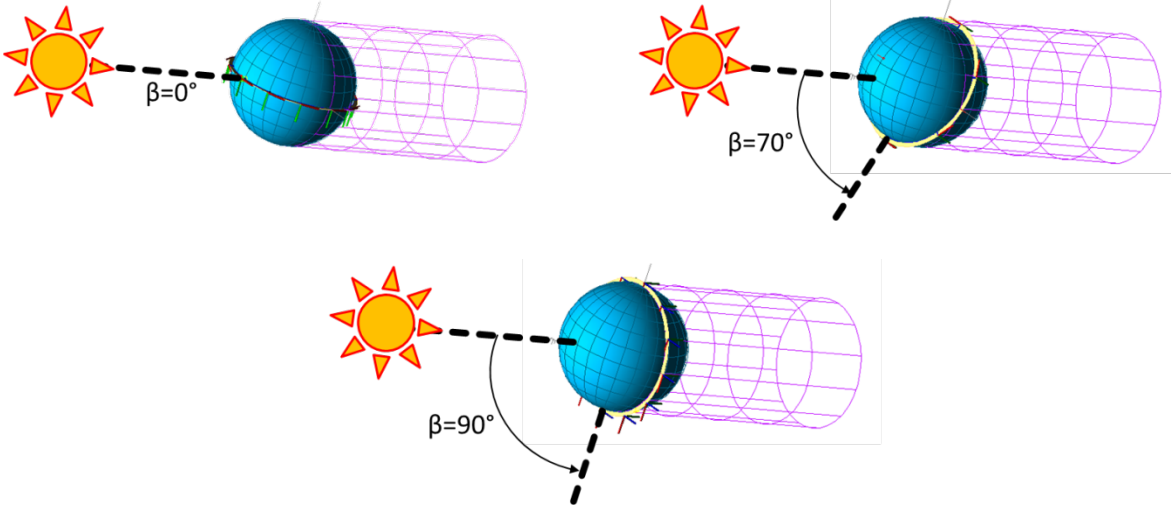

Figure 4. Illustration of bounding orbit cases used for thermal balance points: Hot Beta 0°, Hot Beta 70°, Cold Beta 90°, and Cold Beta 90° Survival.

An iterative process was used in order to determine the appropriate temperature setpoints of the four thermal control surfaces in the chamber, to simulate flight conditions for each of the orbit cases described. First, to get an initial estimate of the appropriate sink temperatures to use, "blocker" surfaces (i.e., small, massless, arithmetic nodes with the same optical properties of the surface they were near) were placed in front of the main radiators of the instrument in the flight model. Theoretically, the temperature these blocker surfaces reached during the flight analysis would serve as the equivalent sink temperature seen by that surface. In reality, the equivalent sink temperatures from the flight model will not be the exact values to use in test, as the test setup is not a perfect representation of space – for example, there is a bounce-back effect in the chamber, wherein heat from the instrument is not totally absorbed (as the shroud is not a perfect black body) and some of the heat is reflected back to the instrument in test, which does not occur in flight. However, the flight sink temperatures serve as a reasonable initial estimate for TVac sink temperatures. As such, these initial sink temperatures were input into the TVac model as respective setpoints for each of the four thermal control surfaces. When the TVac model was run using these setpoints, the instrument temperature and heater power predictions were compared to those of the flight predictions. The goal in this analysis was to have each of the components within 2°C of flight predictions, and each of the heater power predictions within either 0.5 W or 10% of flight predictions. It was noted in advance that some compromises may have to be made, as in many of these cases one thermal control surface is used to drive the temperatures of several instrument components. After this initial estimate with flight sink temperatures, the TVac sink temperatures were refined using hand calculations, as described below. The values of the setpoints were adjusted iteratively until these goals were adequately met.

The following calculations were performed for each of the major components of the instrument at each iteration. The basic radiation heat transfer equation (1) is shown below:

$$Q_{radiation} = A * e * \sigma * \left(T^4 - {T_s}^4\right) \quad (1)$$

If the component was operational but its heaters were turned off during that orbit case, then constant dissipation was assumed and the test and flight heat dissipation could be set equal, as below. By cancelling out the constant area and emissivity of the radiator, as well as the Stefan-Boltzman constant (σ), the desired sink temperature can be solved for as in equation (2):

$$Q_{1,\ test} = Q_{2,\ flight}$$

$$\cancel{A_{component} * e_{component} * \sigma} * \left({T_{1,test}}^4 - {T_{sink1}}^4\right) = \cancel{A_{component} * e_{component} * \sigma} * \left({T_{2,flight}}^4 - {T_{sink2}}^4\right)$$

$$T_{sink2,\ by\ temp} = \sqrt[4]{\left(T_{2,flight}\right)^4 - \left(T_{1,\ test}\right)^4 + (T_{sink1})^4} \quad (2)$$

Where T_{sink1} represents the temperature of the test sink from the previous iteration, and T_{sink2} represents the temperature that the test sink should be set to in the next iteration to achieve more flight-like temperature results for the component.

Alternatively, if the heater power was turned on, the power dissipation would be variable and the above approach could not be used. Instead, a ratio was calculated comparing the amount of heat transferred in test and flight cases, as shown below. Cancelling constants and solving for T_{sink2} yields equation (3):

$$\frac{Q_{2,\ flight}}{Q_{1,\ test}} = \frac{\left({T_{flight}}^4 - {T_{sink2}}^4\right)}{\left({T_{flight}}^4 - {T_{sink1}}^4\right)}$$

$$T_{sink2,\ by\ power} = \sqrt[4]{\left(T_{flight}\right)^4 + \left(\frac{Q_{2,\ flight}}{Q_{1,\ test}}\right)\left[\left(T_{sink1}\right)^4 - \left(T_{flight}\right)^4\right]} \quad (3)$$

Where, similarly, T_{sink1} represents the test sink from the previous iteration, and T_{sink2} represents the value that the test sink should be set to in the next iteration to achieve more flight-like heater power results for the component.

After performing the above hand calculations for major components of ATLAS and iterating with TVac simulation runs, the setpoints for each thermal surface was determined. In the final iteration, the goals were successfully met: nearly all of the components were within 2°C of the flight temperature predictions, and nearly all were within 10% or 0.5W of flight heater power predictions, as shown in Table 1.

Table 1. Results of Setpoint Analysis: Temperature and Heater Power Comparison of Test and Flight Predictions. Note: The difference (Δ) here refers to a subtraction of test value minus flight value.

	HB00		HB70		CB90		CB90 Survival	
Component	ΔT (°C)	ΔQ_{HTR} (%)	ΔT (°C)	ΔQ_{HTR} (%)	ΔT (°C)	ΔQ_{HTR} (%)	ΔT (°C)	ΔQ_{HTR} (%)
PDU I/F*	0.3	0%	-0.7	0%	0.7	0%	0.0	1%
LRS Elec I/F*	1.4	0%	1.7	0%	1.7	0%	0.1	-3%
LRS Opt I/F*	-0.1	13%, 0.3 W	0.0	-7%	0.0	-5%	-0.1	0%
Beam Expander†	-0.7	0%	-0.4	0%	-1.2	0%	-1.4	4%
Telescope Primary‡	0.7	0%	0.6	0%	0.1	-12%, -0.2W	1.1	0%
MEB I/F§	1.1	0%	1.9	0%	1.8	0%	0.2	-6%
DAA Elec I/F§	0.8	0%	1.3	0%	1.1	0%	-0.1	-5%
DAA Optics I/F§	-1.6	0%	-0.3	0%	0.0	0%	0.0	-5%
LHP Liquid Line§	-16.8	0%	-7.9	0%	1.2	32%, 19W	0.1	6%

*Primarily controlled by +X cryo panel

†Primarily controlled by -Y heater panel

‡Primarily controlled by +Z cryo panel

§Primarily controlled by shroud

The one component that did not meet the goal criteria was the Loop Heat Pipe (LHP) Liquid Line, which is the subcooled region of the loop heat pipe on the laser radiator, as shown in the image accompanying Table 1. However, as seen in the table, this component, along with three others – the Main Electronics Box (MEB), the Detector Array Assembly (DAA) Electronics, and the DAA Optics – are all controlled via the shroud. Therefore, a compromise was necessary. It

was decided by the thermal team lead that it was more important to have the electronics boxes and detector arrays at the correct (flight-like) temperatures and heater powers than to have the bottom portion of the laser radiator at the correct temperature and heater power, thus, the LHP liquid line was allowed to be outside of the goal range of flight-like conditions as a necessary compromise. Additionally, it was deemed less important to have the LHP Liquid Line at its flight temperature during the instrument-level test because this item will already be tested as part of a thorough component-level thermal balance test of the Laser Thermal Control System, which is performed prior to the instrument-level test.

A summary of the final setpoints for each thermal control surface, as determined for each orbital case, is shown in Table 2. As a note, the +Z panel was originally intended to be a heater panel, but the required cooling in the CB90° Survival case necessitated a change to a cryo panel.

Table 2. Summary of Setpoints for Thermal Control Surfaces.

	HB00			HB70			CB90			CB90 Survival		
	Flight Sink (°C)	Test Sink (°C)	Test Power (W)	Flight Sink (°C)	Test Sink (°C)	Test Power (W)	Flight Sink (°C)	Test Sink (°C)	Test Power (W)	Flight Sink (°C)	Test Sink (°C)	Test Power (W)
+X Cryo Panel	-47	-76	-92	-63	-108	-97	-101	-138	-83	-94	-119	-59
-Y Heater Panel	-74	110	510	26	135	676	-28	50	259	-84	60	302
+Z Heater Panel	7	32	101	17	23	59	-28	-28	10	-80	-60	-26
Shroud	-78	-100	n/a	-84	-101	n/a	-97	-115	n/a	-85	-105	n/a

Another observation for this section is the comparison of test and flight sink temperatures. Ideally, it is desirable to have sink temperatures that are relatively close to flight sink temperatures to ensure the instrument is tested in a flight-like environment. As seen in Table 2, most of the test sink temperatures seem reasonably close to flight. The exception is the –Y heater panel, which is significantly warmer than the equivalent flight sink temperature. At the time of this analysis, it was likely that there would be optical ground support equipment (GSE) in the chamber located on the –Z side; as a result, the –Y heater panel is used to heat up the –Z side. The effect is that the –Y test sink temperature is much higher than flight. However, as seen in Figure 5, the effect on the structure and optical bench (which are covered with blanketing) is minimal: structure is about 8°C warmer and OB is about 1°C warmer on –Y side.

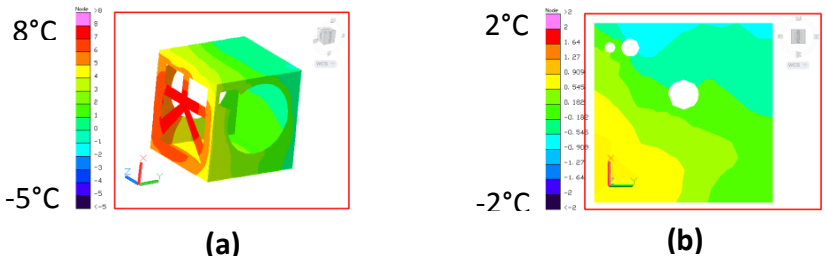

Figure 5. Illustration of temperature differences in HB00 case for structure (a) and OB (b) as a result of having the –Y heater panel warmer than flight sink temperature. (Note: The "difference" plotted here refers to subtraction of test value minus flight value.)

Numerous options are being explored to satisfy multiple subsystems (thermal, optical, etc.), which might enable the –Y sink temperature to become more flight-like. At present, however, the current design is assumed to hold and is used in the subsequent analyses presented here.

STOP ANALYSIS AND RESULTS

The TVac model was then used to generate temperatures for the STOP analysis. The objective during the STOP analysis is to predict the Line of Sight (LOS) pointing error that will occur due to thermal distortions. This LOS error is then analyzed to determine if the error is within pointing requirements and if the error in test is similar to that of flight.

All of the alignment-sensitive optical components are located on the Optical Bench (OB); as such, the OB is the main focus of the STOP analysis.

Figure 6 shows the location of the transmit beam path, as well as the region of the optical bench which is most sensitive to transmit beam errors and receive beam errors. A thermal gradient in these areas, for example, could cause structural deflection which could result in a noticeable effect on the beam path pointing alignment. These are the main areas of interest on the OB.

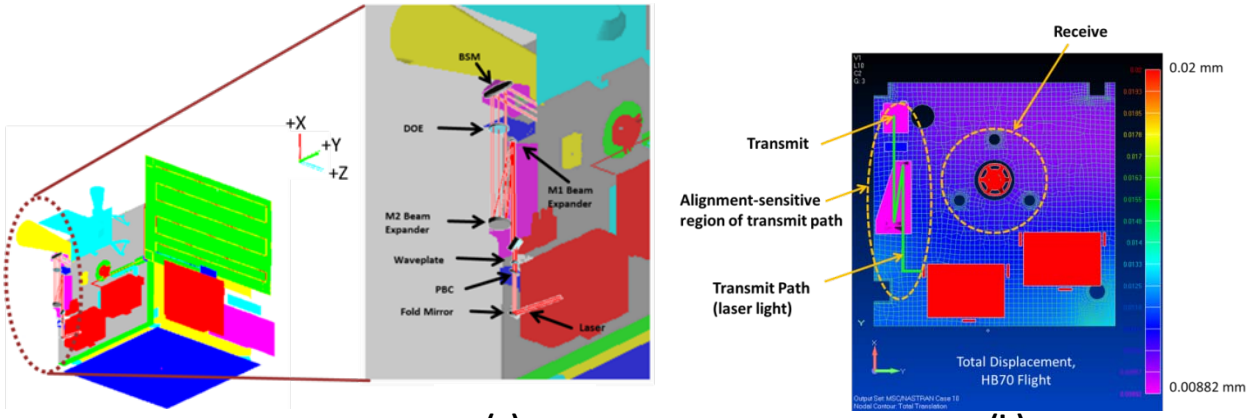

(a) **(b)**

Figure 6. Illustrations of beam path on optical bench, as seen in solid model (a) and Finite Element Model (FEM) (b).

In performing the STOP analysis, the following commonly-used approach was used:

- Generate temperatures
- Map Thermal Desktop (TD) model to FEM model
- Validate mapping (shown in Figure 7)
- Generate displacements
- Generate LOS errors
- Compare results to requirements (shown in Figure 8)

In order to verify that the mapping was performed well, a temperature plot from the thermal model was compared to the (post-mapping) temperature plot of the structural model. This comparison is shown in Figure 7. From this, it is seen that the NASTRAN and Thermal Desktop (TD) temperatures for the Optical Bench are in agreement, which implies that the TD nodes have been mapped to the NASTRAN nodes successfully.

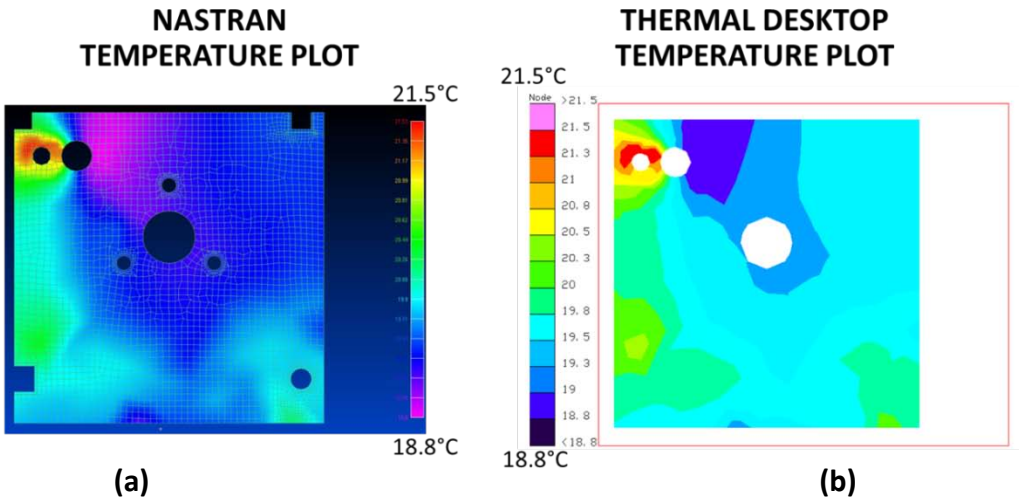

Figure 7. Mapping verification: temperature comparison between NASTRAN plot (a), and Thermal Desktop plot (b), for HB70 case.

The final step in the STOP analysis is evaluating the LOS pointing errors that are due to thermal distortions of the Optical Bench. As an example, the results for the HB70 case are shown in Figure 8. From this, it is seen that the LOS test and flight predictions are each well within the requirement of 100 µrad of LOS error. The results for the remaining cases are shown in Appendix D.

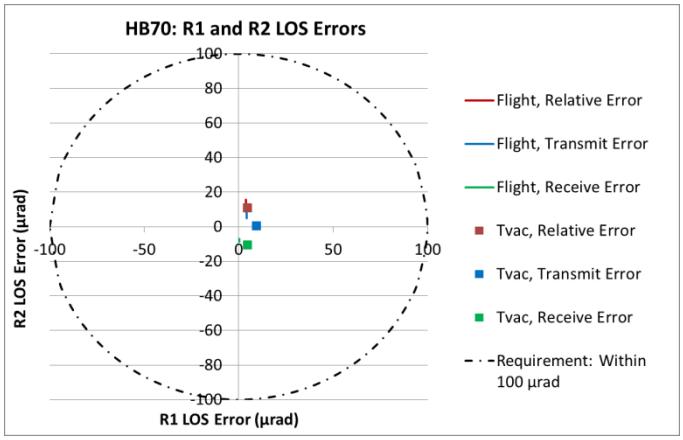

Figure 8. LOS results for HB70: Error is within the requirement.

A detailed view of the LOS error results is shown in Figure 9. In this plot, the LOS error of the transmit beam is shown in blue, the LOS error of the receiving beam is shown in green, and the relative error between the transmit and receive beams (ie, the total error) is shown in red. The horizontal axis represents the amount of rotational error of the beam about the +X axis of the instrument; this rotational error is called R1. Similarly, the rotational error about the +Y axis of the instrument is called R2. The rotation about the +Z axis (R3) is neglected in this LOS analysis as the beams are pointing along the +Z direction, and thus a rotation about the +Z axis would not cause an LOS pointing error. A reference diagram, showing R1, R2, and R3, as well as the X, Y, and Z axes of the instrument, is shown in Figure 10.

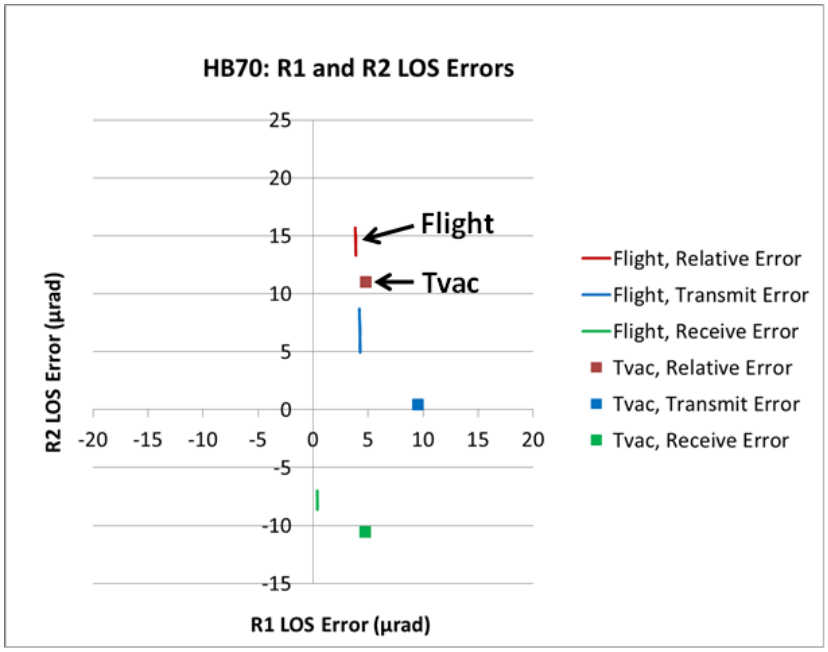

Figure 9. Detailed view of LOS results for HB70.

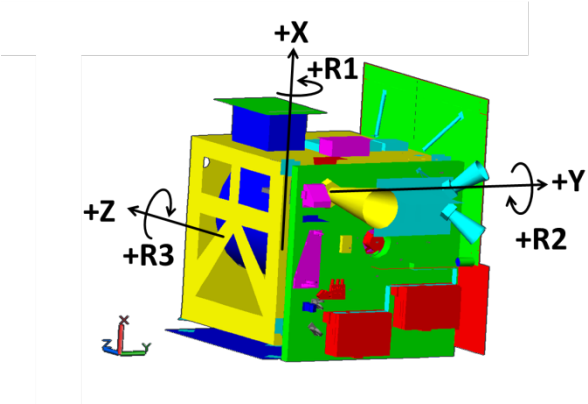

Figure 10. Diagram showing axes of rotations relative to ATLAS reference frame.

In order to calculate the relative (total) error between the transmit and receive beams, vector subtraction is performed. This is illustrated on the graph in Figure 11, as well as in physical space in Figure 12. (As a note, the diagram in Figure 12 diagram shows an exaggerated view of a hypothetical error.) In physical space, as seen in Figure 12, the receiving beam is coming into the telescope (along the –Z direction, with some error). For ease of computing with optics equations, it is desirable to take both the transmit beam and the receive beam with respect to the +Z axis when calculating the respective LOS errors of each beam; thus, the receiving beam is flipped 180 degrees, to become R'. Once the LOS error of each beam is computed, the relative (total) error is found by taking the difference between the transmit beam error and the receive beam error (ie, performing vector subtraction). This provides a result for the total (relative) error, which is shown in red.

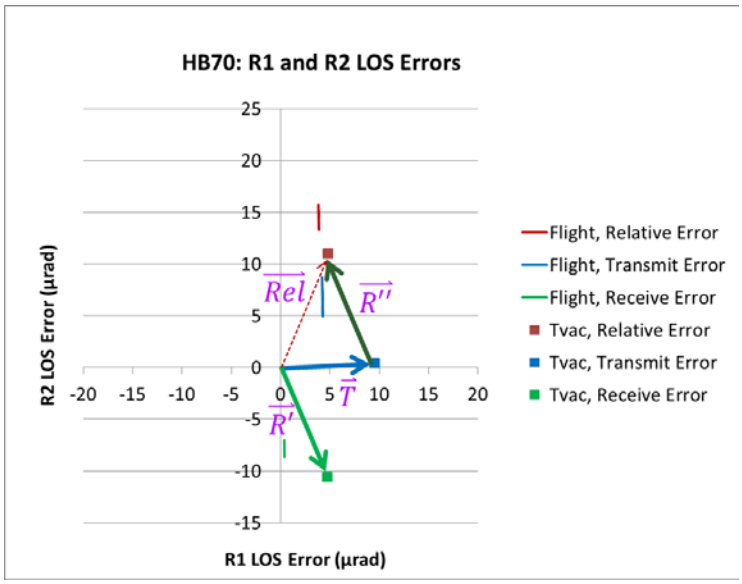

Figure 11. Vector subtraction of transmit and receive beam LOS errors is used to compute the relative (total) error between the transmit and receive beams.

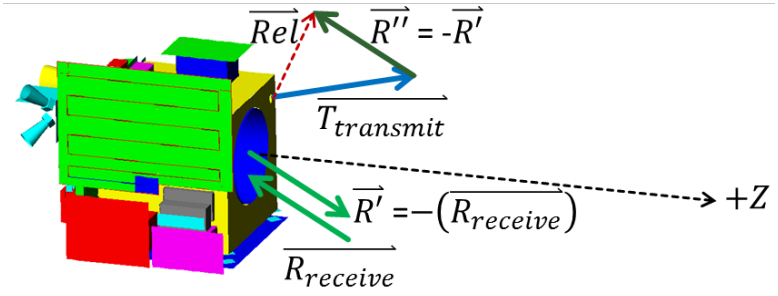

Figure 12. Illustration of the transmit, receive, and relative pointing errors in physical space. (Note: This illustration uses hypothetical and exaggerated LOS errors for each beam, to serve as a visual example.

As described earlier, the flight LOS and test LOS predictions in Figure 9 are very close to each other; however, they not identical. Ideally, these would be the same value, as it is desirable to simulate flight as closely as possible. In investigating this, a temperature plot comparison was created for the Optical Bench (OB), comparing flight and test temperatures. As seen in Figure 13, the temperature distributions are slightly different in flight than in the test chamber for the HB70 case. The difference is small, approximately 1°C warmer on the -Y side of the optical bench and 1°C cooler on the +X and +Y sides. Physically, this makes sense, as there is a heater panel near the –Y side of the OB in the chamber, and similarly the +X side is close to a cryo panel and the +Y side sees a cold shroud. Therefore, the temperature difference between test and flight seems reasonable. In addition to looking at a temperature map, a displacement map was also analyzed. Figure 13 shows the total displacement of nodes in the Optical Bench, for test and flight. Thus, as seen in Figure 13, the thermal distortion is different between test and flight. Therefore, it is reasonable that the flight LOS error will differ slightly from the test LOS error, as is seen in Figure 9.

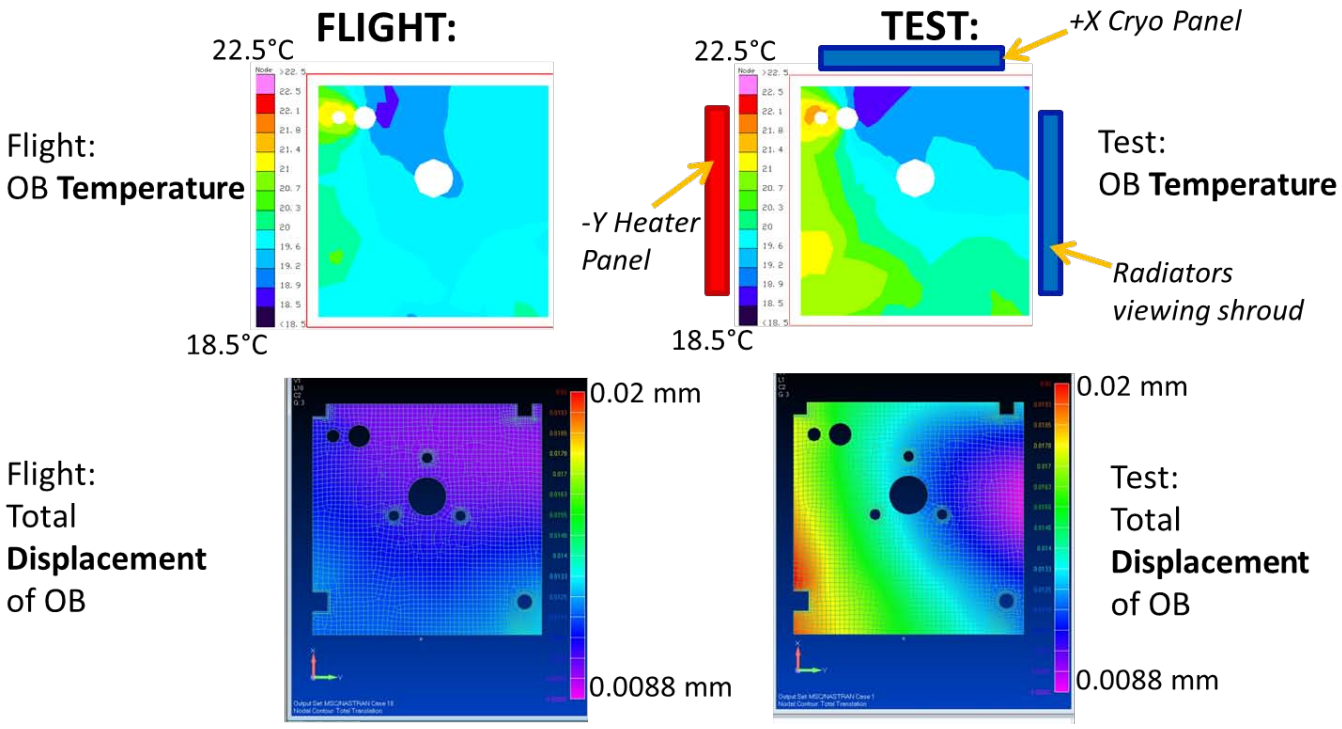

Figure 13. Comparison between flight and test results for temperature and displacement. The upper plots represent temperature distribution on the OB for flight (left) and test (right). The lower plots show total displacement of the OB for flight (left) and test (right).

The second aspect of the LOS plot that was investigated was the orbit variation observed for the flight case. By inspecting the timestep where the greatest LOS error occurred, as well as the timestep where the least LOS error occurred, it was possible to ascertain which parts of the orbit result in the greatest pointing error, and which the least. As seen in Figure 14, the part of the orbit with the least pointing error is the top part of the orbit, where the optical bench is pointing away from the sun and has a view to deep space; the optical bench is colder here, as can be seen by the temperature map shown near that part of the orbit. Similarly, the part of the orbit that exhibits the largest amount of pointing error occurs at the bottom of the orbit, where the optical bench has a slight view to the sun; the OB is warmer here, and has a slightly greater thermal gradient around the transmit beam region, as shown in the temperature map near that part of the orbit. This increase in thermal gradient may lead to greater pointing error, as is seen in the graph in Figure 14.

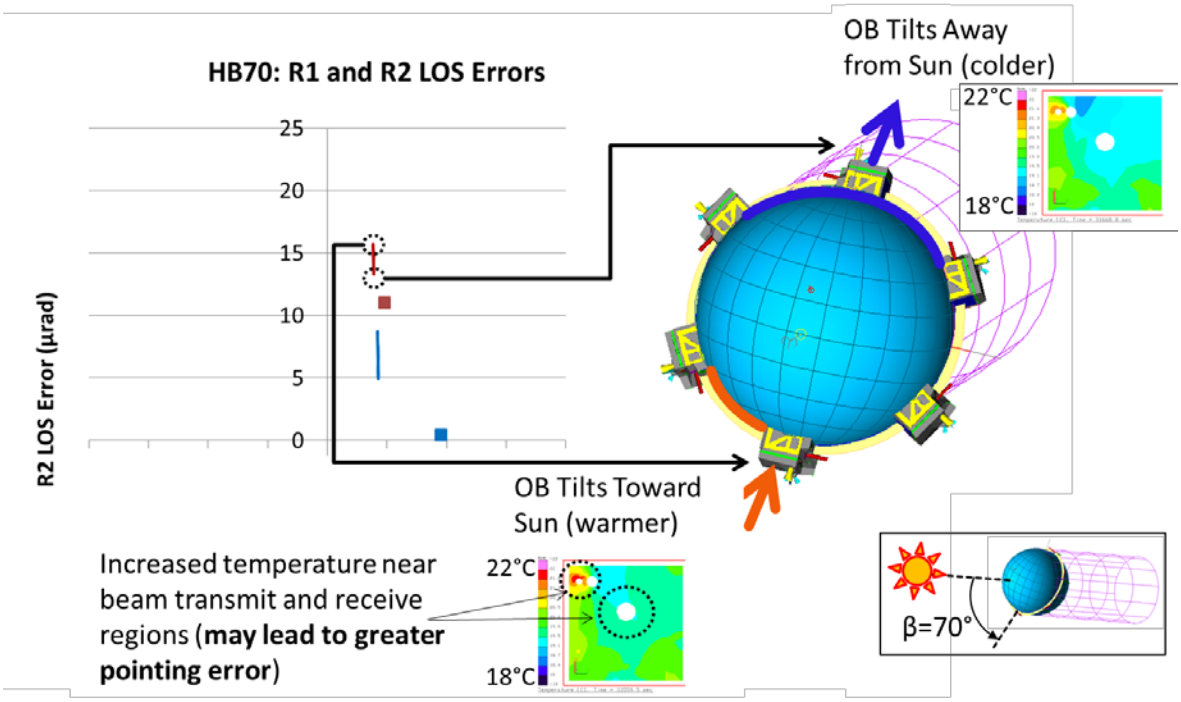

Figure 14. Orbit variation contributes to LOS increase.

The last aspect investigated for the STOP analysis was a comparison of temperatures of the OB for flight and test cases, performed for each of the operational orbit cases analyzed (HB00, HB70, and CB90). A map of the temperature difference was created for each case; as an example, the results of HB70 are shown in Figure 15. As can be seen in this map, temperatures are a little warmer on the –Y side (which is close to a heater panel) and a little cooler than flight on the +X side and +Y side (which are close to a cryo panel and the shroud, respectively, in test). This map, which represents test temperatures minus flight temperatures, indicates that the test

predictions are within +/- 2°C of flight predictions. This is true for all three operational cases. The results for the remaining cases are shown in Appendix E.

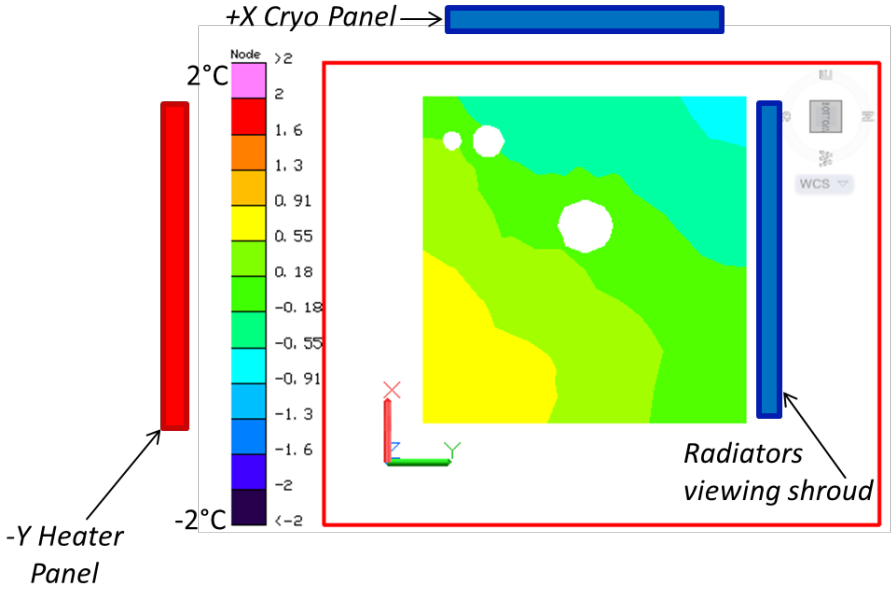

Figure 15. HB70 Case: Comparison of test and flight temperature predictions for Optical Bench, plotting the difference in temperature. (Note: "Difference" here refers to subtraction of test temperature minus flight temperature.)

In summary for this section, the LOS analysis verified that ATLAS will perform within pointing requirements both during flight and test, that the pointing error is within 100 µrad. Also, it was verified that flight and test LOS errors are very close to each other, within approximately 15 µrad. Lastly, it was verified that the temperature of the optical bench in TVac is within +/-2°C of the flight prediction, which is within testing tolerance.

CONCLUSIONS AND FUTURE WORK

The test setup has been designed such that the ATLAS instrument test predictions for temperature and heater power are close to those that are expected for flight, using this test setup. It was also noted that the test sink and flight sink differ for the –Y side of the instrument, and that it might be desirable (as future work) to investigate another approach for simulating the flight sink on that side. Also, a STOP analysis was performed, the results of which indicate that ATLAS will be able to perform within the pointing requirement when in the chamber, and that test and flight pointing predictions are similar.

Performing a STOP analysis for an instrument in its TVac test configuration was a novel aspect of this work, as a new application of an existing process. Historically, STOP analyses are typically performed only for flight configurations. However, due to the unusually tight pointing requirements of ATLAS, and the consequent need to conduct performance testing of the instrument's active alignment system while in TVac, it was necessary for ATLAS to perform this unique STOP analysis for the test configuration of the instrument as well. Another innovative aspect of this test is that it presents the opportunity to verify the STOP model, which is not usually possible. It is achievable in this case, however, because the active alignment system on ATLAS will be operating and collecting data during the thermal balance points of the TVac test. As such, the actual alignment error that occurs while ATLAS is in the chamber can be measured and compared to the alignment error predicted by the STOP analyses performed for the TVac setup, to verify how close the model predictions of the STOP analysis are to actual measurements.

For future work, a systems-level decision will need to be made regarding the setup of the –Y side in the chamber. Depending on the outcome of this decision, the –Y heater panel may be split into two panels, and/or a heater panel may be added to the –Z side, or the design of the test setup may be carried out as-is. If either of the first two options is selected, then this analysis will be re-done to reflect the updated –Y panel configuration.

Additional future work will include developing further specifications for the heater and cryo panels, such that the hardware can either be fabricated, or existing panels can be used. If the latter, then this analysis would be re-done to account for actual dimensions of existing heater and cryo panels (which are likely to be slightly different than the dimensions assumed for this analysis).

Once the test design is finalized, the STOP analysis will be performed again to reflect the changes made. In addition to an updated test design, this STOP analysis would also include updates to the structural model, which would include the spacecraft and the spacecraft interface plate (which were omitted from structural model in the previous STOP analysis), as well as a more detailed analysis of thermal distortions within each of the optical components on the optical bench. These combined will result in a set of updated pointing error predictions for flight as well as test. The results of the test predictions will be used as inputs in the thermal vacuum test plan for the ATLAS instrument-level test. Also, once this thermal vacuum test is performed, the pointing data collected during the test can be used to verify the STOP analysis predictions made prior to the test; this is unique, in that normally it is not possible to verify the STOP analysis. ATLAS will be able to do this, however, as it has an onboard active alignment system that will be tested in TVac, and shall record data that can be used for verification purposes.

In summary, the ATLAS thermal vacuum test will need to simulate the flight environment thermally, as well as mechanically and optically, in that this unique instrument has unusually challenging pointing requirements which must be met during TVac testing. The work presented

in this paper has provided a viable setup for this thermal vacuum test, and has provided insights and guidance into how this test will be performed in 2015.

ACKNOWLEDGEMENTS

Many thanks are due to the following people, who provided wisdom, guidance, and technical support on this project: David Steinfeld, Matt Garrison, Deepak Patel, Sheila Wall, Laurie Seide, Lun Xie, Hume Peabody, Kan Yang, John Hawk, Juan Rodriguez-Ruiz, Richard D'Antonio, and Luis Ramos-Izquierdo. Appreciation also goes to the following people, who provided feedback on the presentation of the completed work: Dan Nguyen, Wes Ousley, Carol Mosier, Justin Brannan, Kevin Fisher, Ron Jones, Eduardo Rodriguez, Rivers Lamb, Elaine Lin, Brian Simpson, Joe Bonafede, and Sassan Yerushalmi.

REFERENCES

[1] "ICESat-2 Home," National Aeronautics and Space Administration, Jun. 28, 2012, http://icesat.gsfc.nasa.gov/icesat2/ [Accessed July 9, 2012].

[2] "ICESat-2", Orbital Sciences Corporation, 2012, http://www.orbital.com/SatellitesSpace/ScienceTechnology/ICESat-2/ [Accessed July 9, 2012]

[3] Martino, Tony, "ATLAS iPDR: Section A6," NASA Goddard Space Flight Center, Greenbelt, MD, Nov. 2011.

[4] "ICESat-2: Science Activities," National Aeronautics and Space Administration, July 1, 2010, http://icesat.gsfc.nasa.gov/icesat2/science.php [Accessed July 9, 2012].

[5] Garrison, Matthew, "ICESat-II Project ATLAS Thermal Balance and Thermal Vacuum Test Plan Rev(-)," ICESat-2-ATSYS-PLAN-1045, NASA Goddard Space Flight Center, June 8, 2012.

[6] "Facilities: T/V Facility 238 (12' x 14')," National Aeronautics and Space Administration, Jun. 23, 2010, http://mscweb.gsfc.nasa.gov/549web/5494web/facility/fac238.htm [Accessed July 10, 2012].

APPENDIX A. NOMENCLATURE

AMCS	=	Alignment Monitoring and Control System
ATLAS	=	Advanced Topographic Laser Altimeter System
β	=	Beta angle
BDF	=	Bulk Data File
BSM	=	Beam Steering Mechanism
CB	=	Cold Beta
DAA	=	Detector Array Assembly
DOE	=	Diffractive Optical Element
FOV	=	Field of View
GLAS	=	Geoscience Laser Altimeter System
GSE	=	Ground Support Equipment
GSFC	=	Goddard Space Flight Center
HB	=	Hot Beta
ICESat-2	=	Ice, Cloud, and land Elevation Satellite-2
I/F	=	Interface
IR	=	Infrared
LHP	=	Loop Heat Pipe
LOLA	=	Lunar Orbiter Laser Altimeter
LOS	=	Line of Sight
LRS	=	Laser Reference System
LSA	=	Laser Sampling Assembly
MEB	=	Main Electronics Box
MLA	=	Mercury Laser Altimeter

MLI	=	Multi-Layer Insulation
MOLA	=	Mars Orbiter Laser Altimeter
NASTRAN	=	NASA Structural Analysis
OB	=	Optical Bench
PBC	=	Polarizing Beam Combiner
PDU	=	Power Distribution Unit
PIP	=	Professional Intern Program
PRF	=	Pulse Repetition Frequency
S/C	=	Spacecraft
SCIF	=	Spacecraft Interface
STOP	=	Structural Thermal Optical Performance analysis
TD	=	Thermal Desktop
TVac	=	Thermal vacuum

APPENDIX B. REFERENCE DIAGRAMS

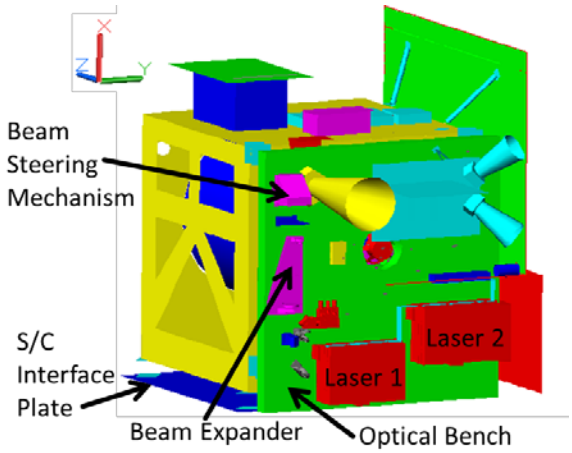

Figure 16. Diagram of ATLAS, with several components labeled.

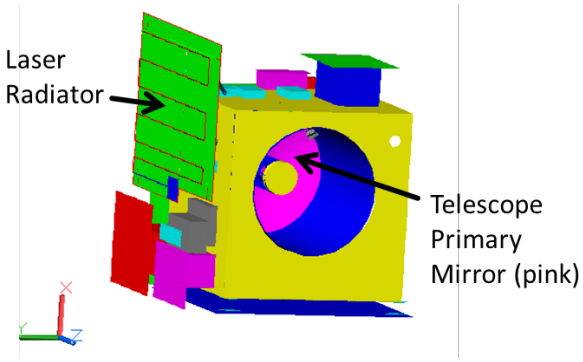

Figure 17. Diagram of ATLAS, with additional components labeled.

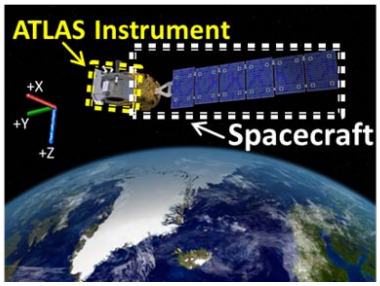

Figure 18. Visualization of ATLAS and spacecraft in orbit.

APPENDIX C. HEAT MAPS

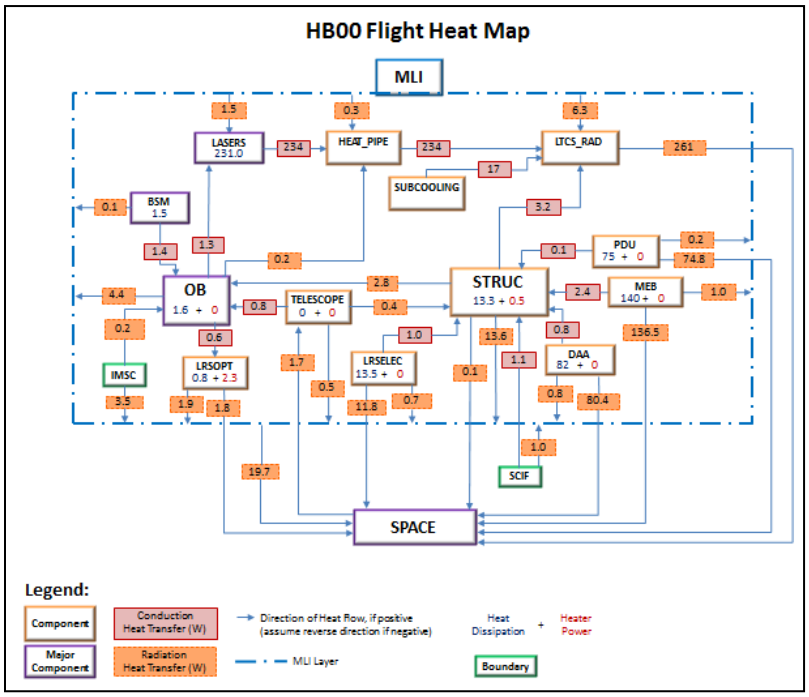

Figure 19. HB00 flight heat map.

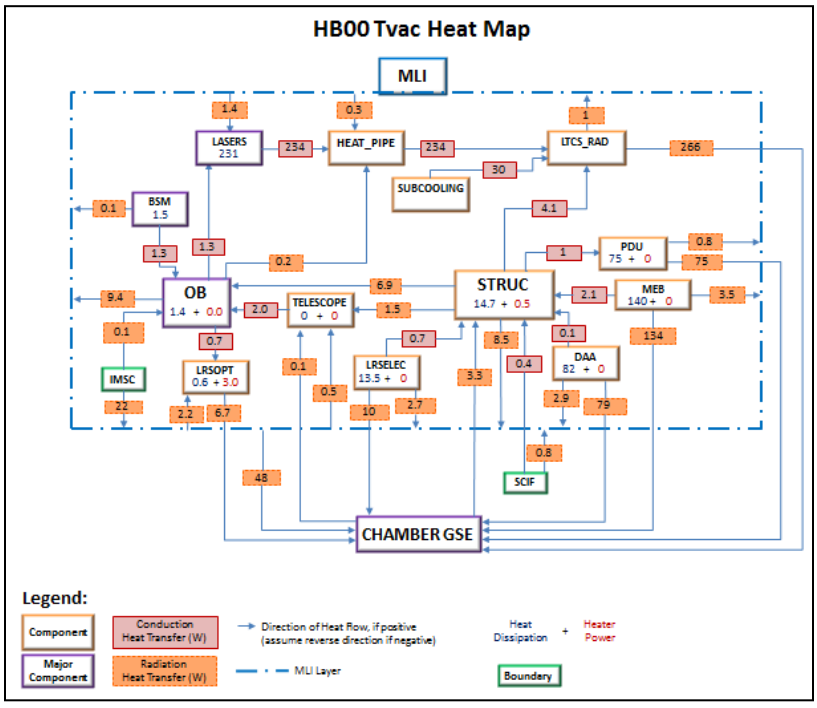

Figure 20. HB00 TVac heat map.

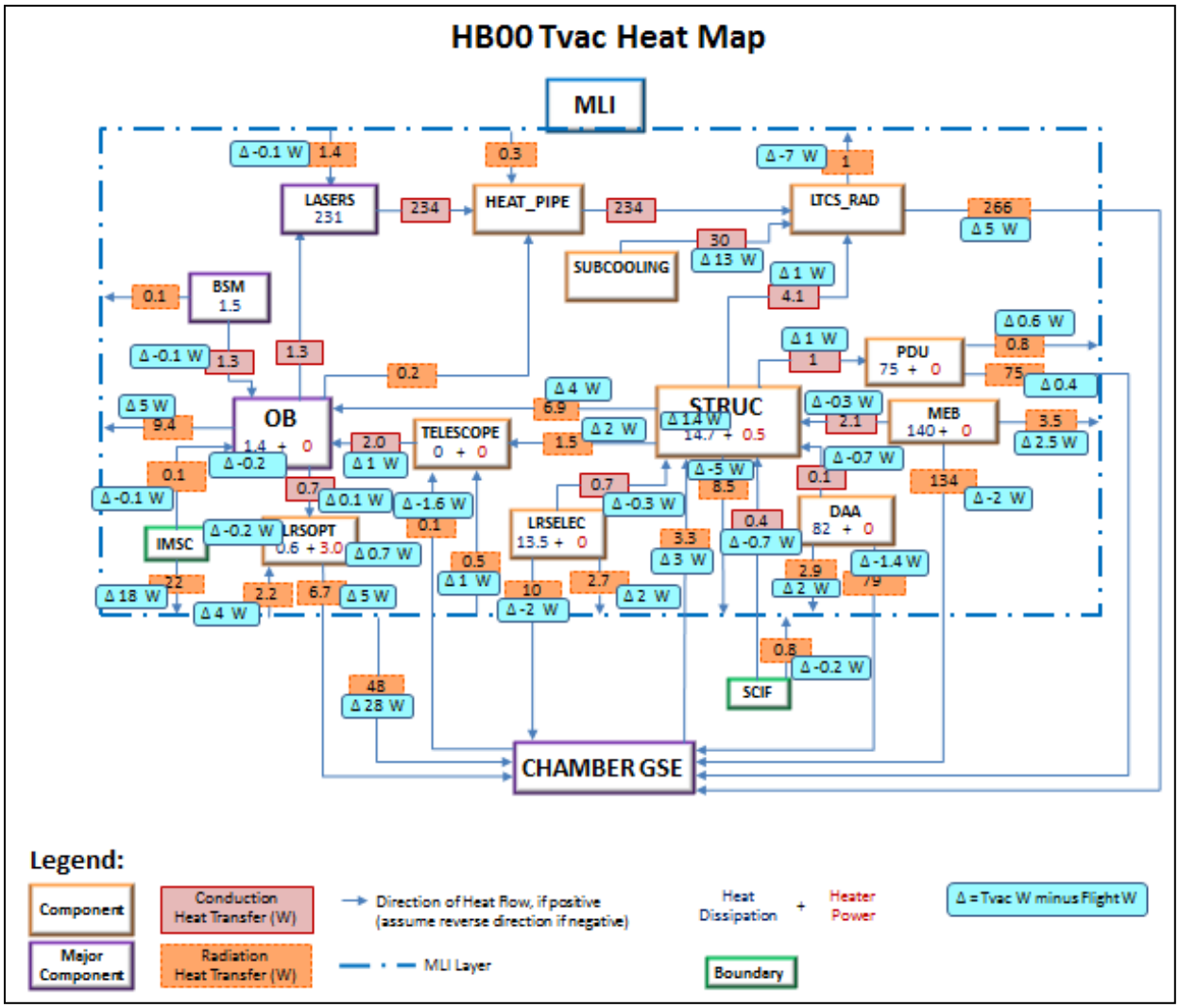

Figure 21. HB00 TVac heat map, showing comparison to flight. Note: the blue boxes represent the difference between test and flight (where "difference" is computed by test value minus flight value).

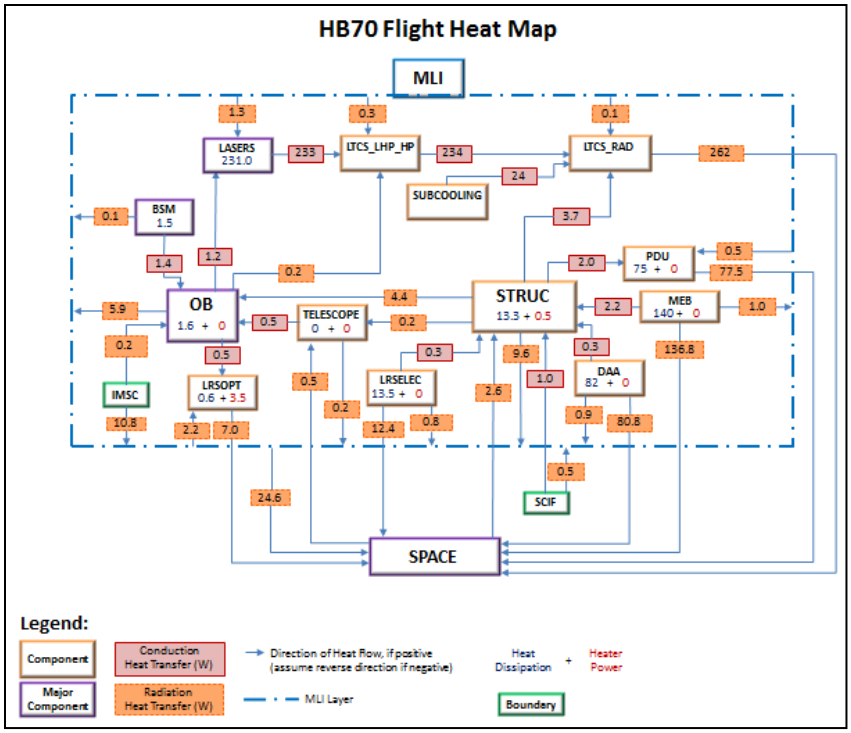

Figure 22. HB70 flight heat map.

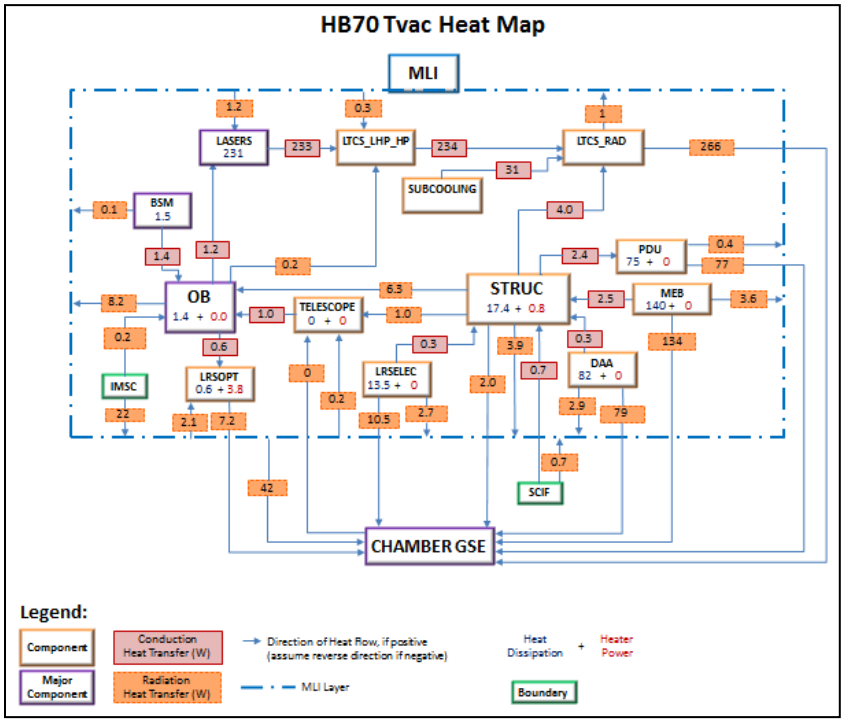

Figure 23. HB70 TVac heat map.

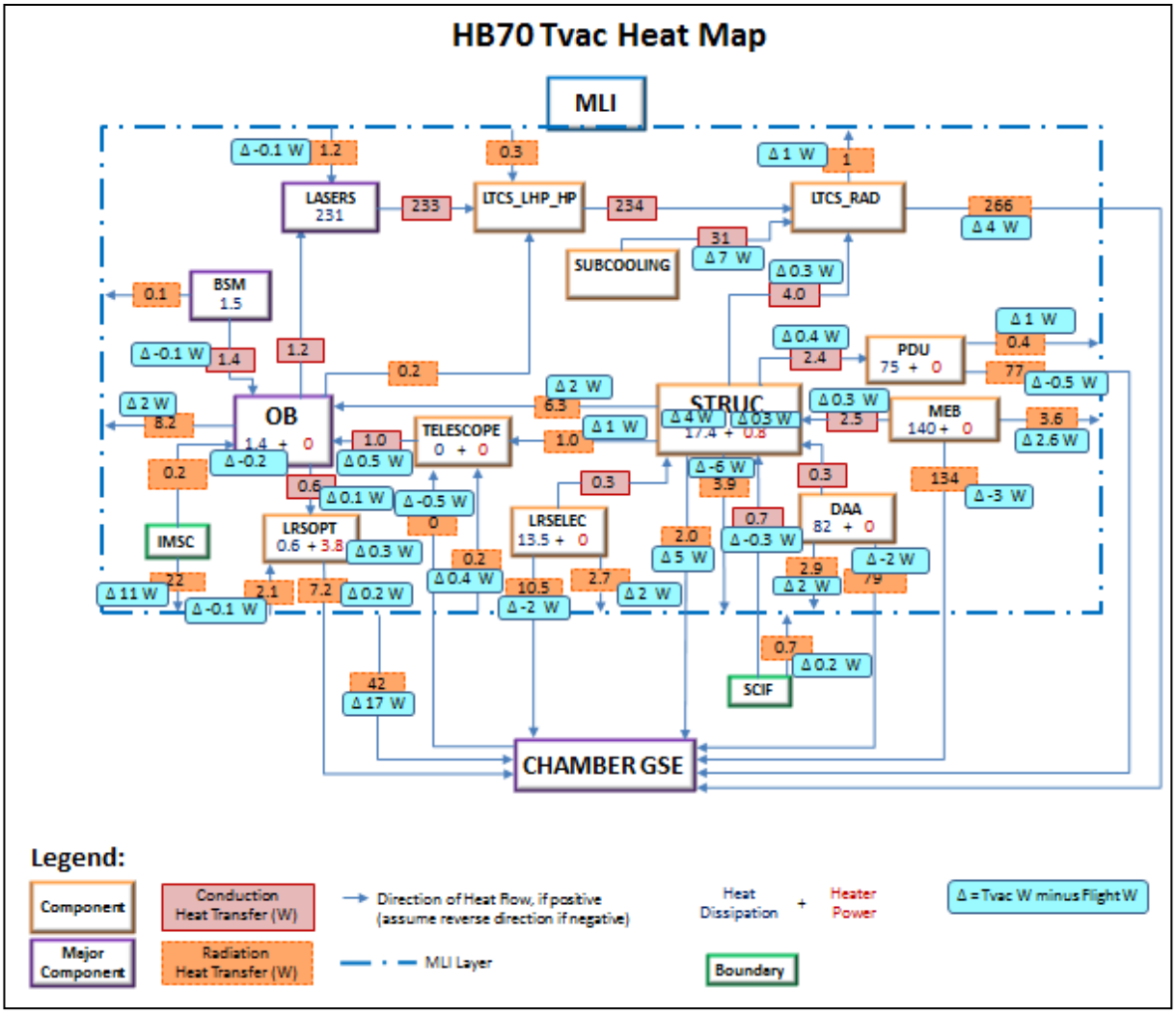

Figure 24. HB70 TVac heat map, showing comparison to flight. Note: the blue boxes represent the difference between test and flight (where "difference" is computed by test value minus flight value).

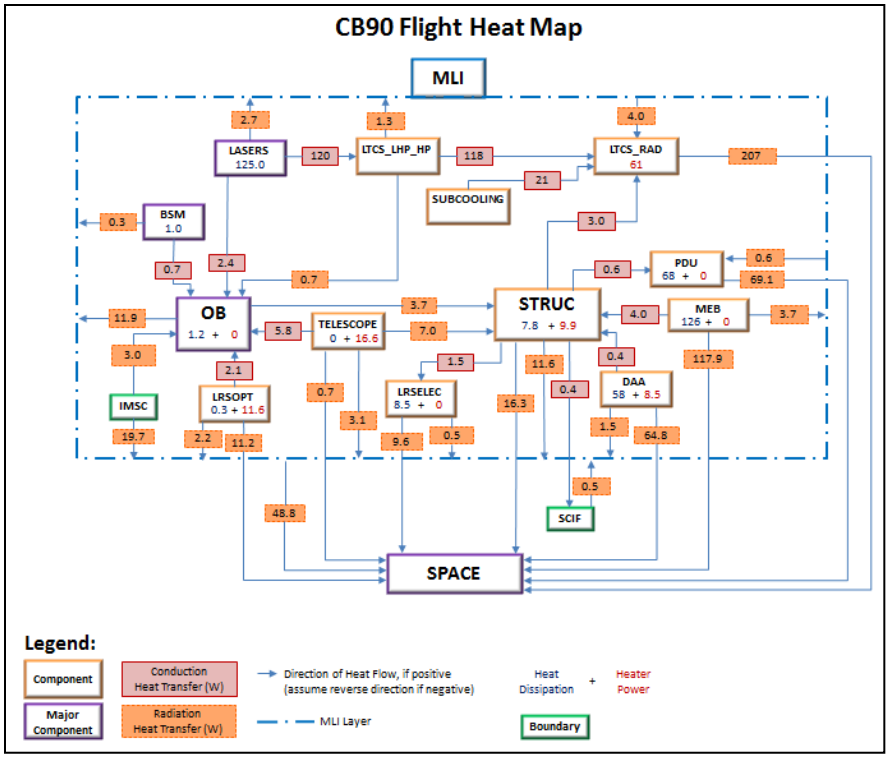

Figure 25. CB90 flight heat map.

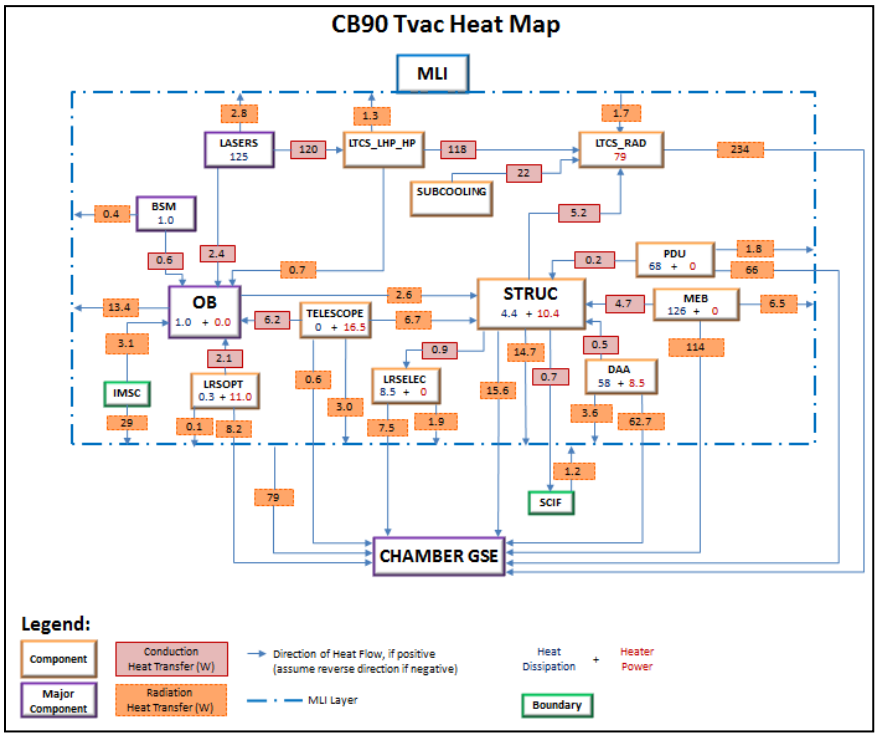

Figure 26. CB90 TVac heat map.

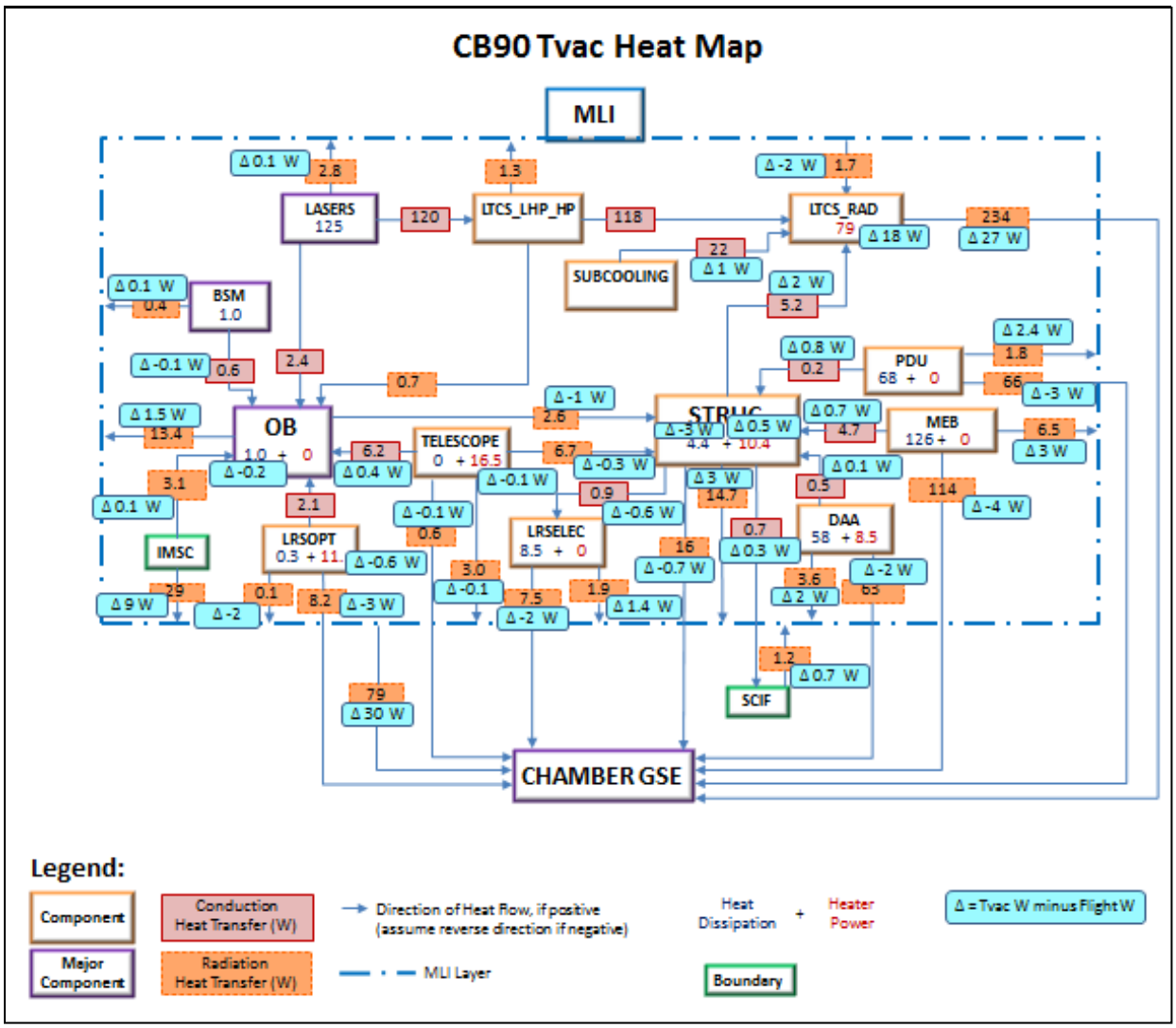

Figure 27. CB90 TVac heat map, showing comparison to flight. Note: the blue boxes represent the difference between test and flight (where "difference" is computed by test value minus flight value).

APPENDIX D. LOS ERRORS

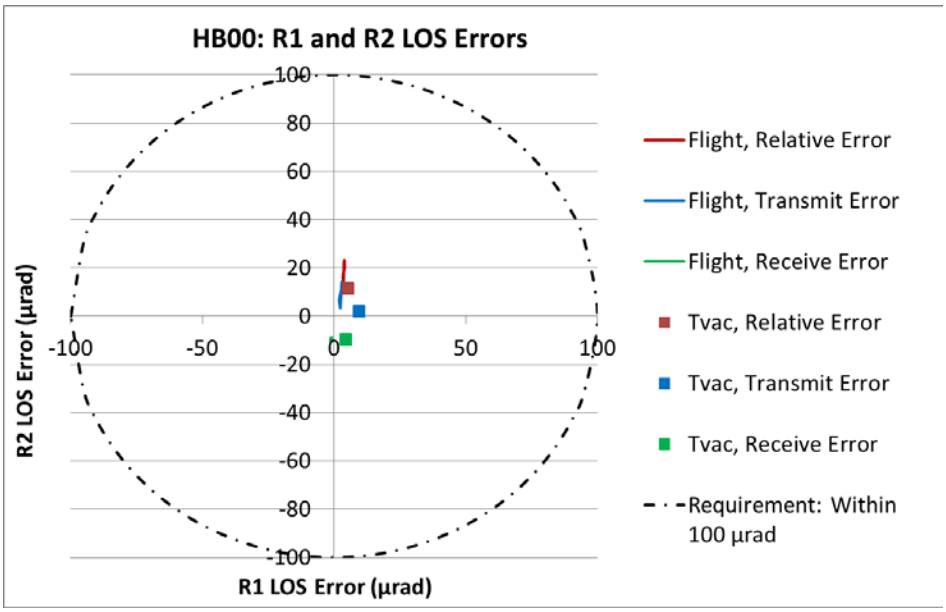

Figure 28. LOS results for HB00: Error is within the requirement.

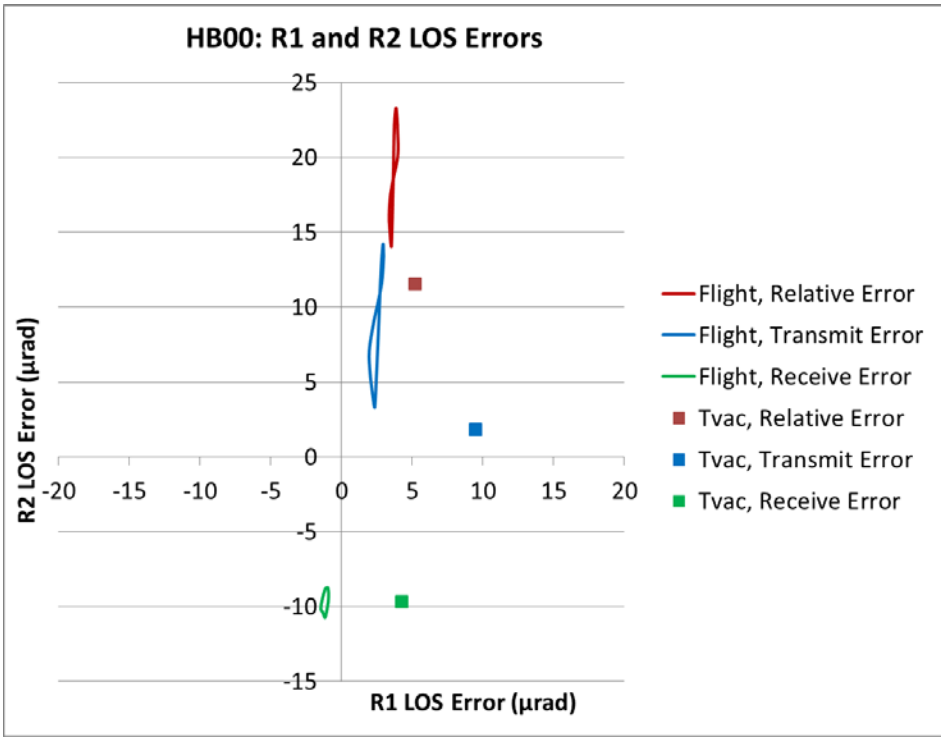

Figure 29. LOS results for HB00, detailed view.

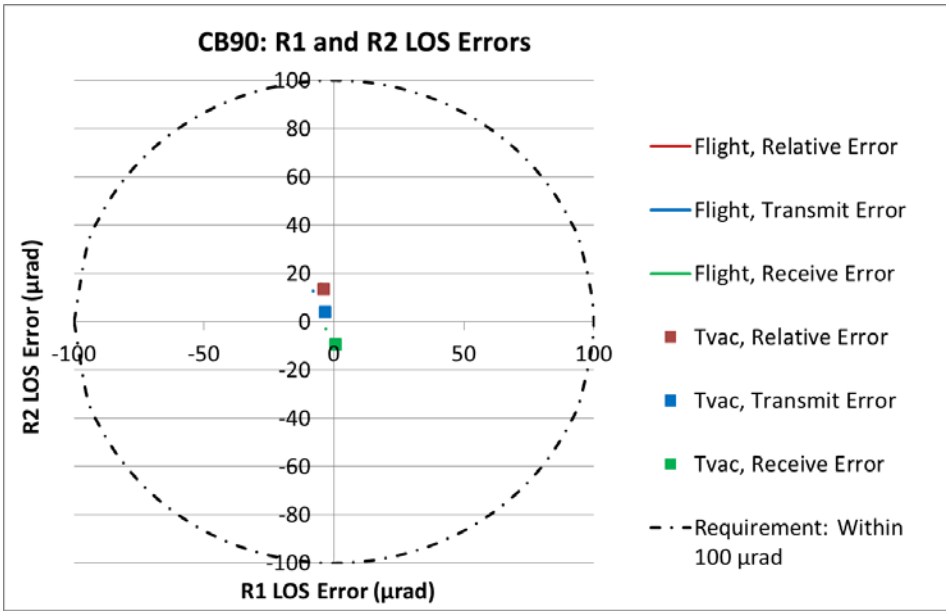

Figure 30. LOS results for CB90: Error is within the requirement.

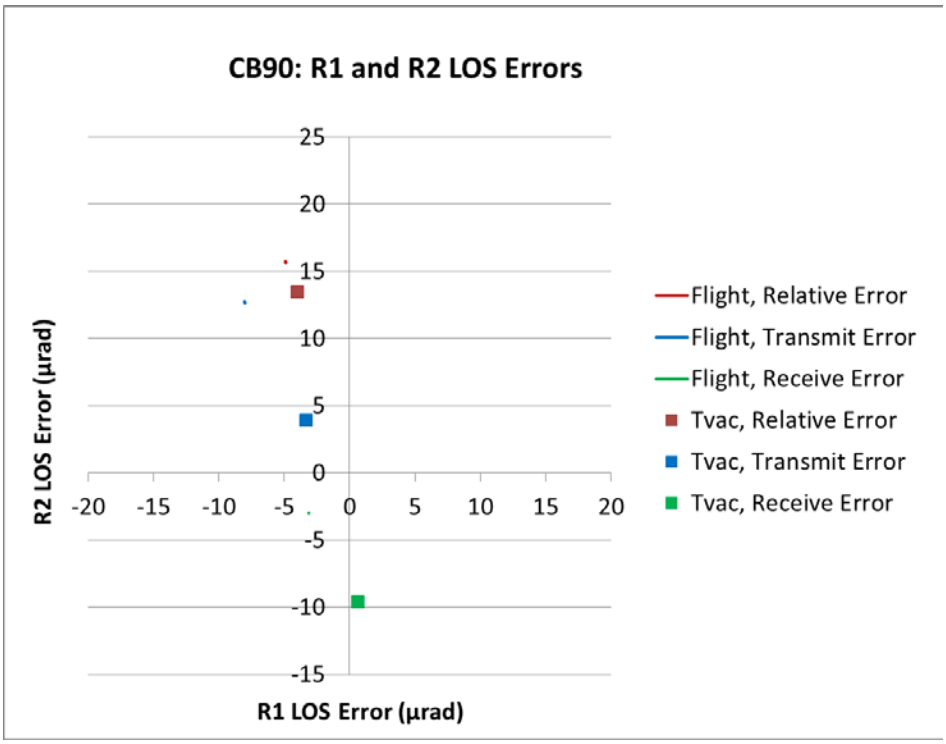

Figure 31. LOS results for CB90, detailed view.

APPENDIX E. OPTICAL BENCH TEMPERATURE DIFFERENCE PLOTS

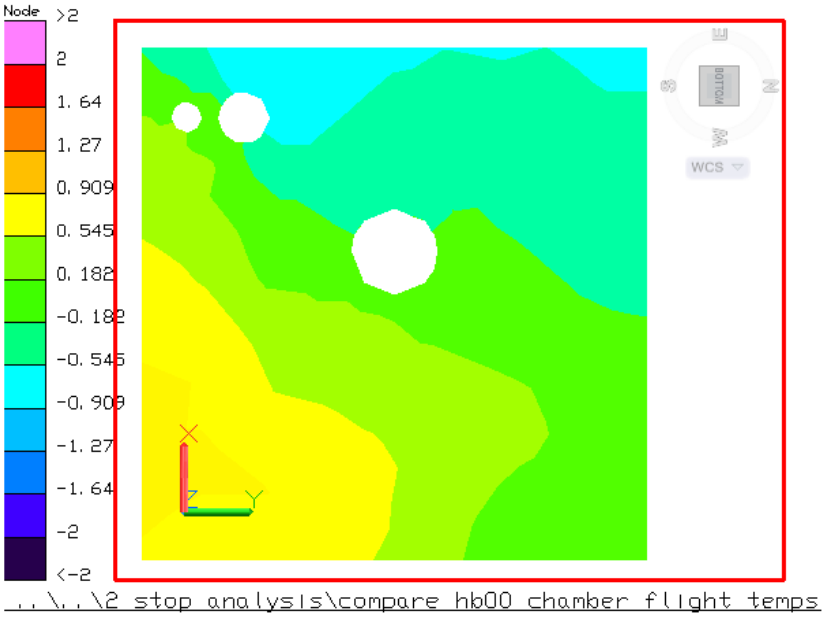

Figure 32. HB00 Case: Comparison of test and flight temperature predictions for Optical Bench, plotting the difference in temperature. (Note: "Difference" here refers to subtraction of test temperature minus flight temperature.)

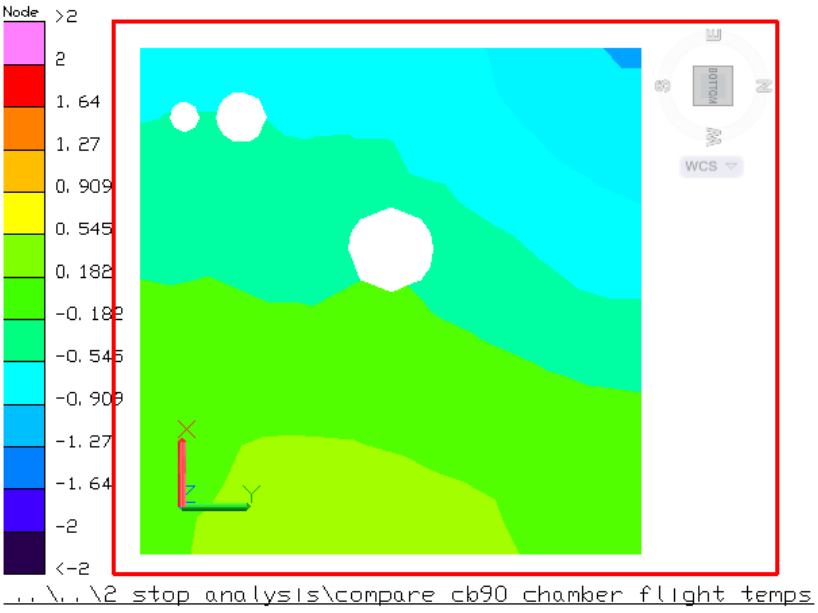

Figure 33. CB90 Case: Comparison of test and flight temperature predictions for Optical Bench, plotting the difference in temperature. (Note: "Difference" here refers to subtraction of test temperature minus flight temperature.)